

OPTIMIZATION OF GRAPHENE SYNTHESIS BY ELECTROCHEMICAL  
EXFOLIATION OF GRAPHITE

A THESIS SUBMITTED TO  
THE GRADUATE SCHOOL OF NATURAL AND APPLIED SCIENCES  
OF  
MIDDLE EAST TECHNICAL UNIVERSITY

BY

VAHIT KURT

IN PARTIAL FULFILLMENT OF THE REQUIREMENTS  
FOR  
THE DEGREE OF MASTER OF SCIENCE  
IN  
METALLURGICAL AND MATERIALS ENGINEERING

DECEMBER 2019



Approval of the thesis:

**OPTIMIZATION OF GRAPHENE SYNTHESIS BY ELECTROCHEMICAL  
EXFOLIATION OF GRAPHITE**

submitted by **VAHIT KURT** in partial fulfillment of the requirements for the degree  
of **Master of Science in Metallurgical and Materials Engineering Department,**  
**Middle East Technical University** by,

Prof. Dr. Halil Kalıpçılar  
Dean, Graduate School of **Natural and Applied Sciences**

\_\_\_\_\_

Prof. Dr. Cemil Hakan Gür  
Head of Department, **Met. and Mat. Eng.**

\_\_\_\_\_

Prof. Dr. M. Kadri Aydınol  
Supervisor, **Met. and Mat. Eng., METU**

\_\_\_\_\_

Assoc. Prof. Dr. Göknur Büke  
Co-Supervisor, **Mat. Science and Nanotechnology Eng.,  
TOBB ETÜ**

\_\_\_\_\_

**Examining Committee Members:**

Prof. Dr. Tayfur Öztürk  
Metallurgical and Materials Engineering, METU

\_\_\_\_\_

Prof. Dr. M. Kadri Aydınol  
Met. and Mat. Eng., METU

\_\_\_\_\_

Prof. Dr. İshak Karakaya  
Metallurgical and Materials Engineering, METU

\_\_\_\_\_

Prof. Dr. Arcan Dericioğlu  
Metallurgical and Materials Engineering, METU

\_\_\_\_\_

Assoc. Prof. Dr. Ziya Esen  
Materials Science and Engineering, Çankaya University

\_\_\_\_\_

Date: 10.12.2019

**I hereby declare that all information in this document has been obtained and presented in accordance with academic rules and ethical conduct. I also declare that, as required by these rules and conduct, I have fully cited and referenced all material and results that are not original to this work.**

Name, Surname: Vahit Kurt

Signature:

## **ABSTRACT**

### **OPTIMIZATION OF GRAPHENE SYNTHESIS BY ELECTROCHEMICAL EXFOLIATION OF GRAPHITE**

Kurt, Vahit

Master of Science, Metallurgical and Materials Engineering

Supervisor: Prof. Dr. M. Kadri Aydınol

Co-Supervisor: Assoc. Prof. Dr. Göknur Büke

December 2019, 88 pages

Graphene is a one atom thick allotrope of carbon that is a honeycomb lattice of carbon atoms. Graphene has a lot of extraordinary properties and these properties cause increasing of interest on it. In addition to high specific surface area, high transparency, high strength, graphene is the material that has best electrical conductivity ever. These properties make graphene a suitable candidate for a lot of applications. Since its discovery, a lot of research has been done about how to produce graphene and how to use it efficiently but researchers are still not being able to produce graphene at large amounts. Therefore, graphene suffers from having high prices and can only be used for some special applications.

In this study, graphene was synthesized by electrochemical exfoliation of graphite which is one of the most cost effective ways to produce high quality graphene with high production rate. In this method, a potential difference is applied between the electrodes (either of which is graphite) in an electrolytic cell and graphene sheets are exfoliated from graphite electrode. In this study, process parameters like applied potential, type of electrolyte and electrolyte additives and cell geometry were optimized to produce high quality graphene with high yield. Synthesized graphene

was characterized using SEM, EDS, TEM, XRD, AFM, BET, FTIR and Raman spectroscopy.

Keywords: Graphene, electrochemical exfoliation, electrolyte, characterization

## ÖZ

### GRAFİTİN ELEKTROKİMYASAL YAPRAKLANMA YÖNTEMİ KULLANILARAK SENTEZİNİN OPTİMİZE EDİLMESİ

Kurt, Vahit  
Yüksek Lisans, Metalurji ve Malzeme Mühendisliği  
Tez Danışmanı: Prof. Dr. M. Kadri Aydınol  
Ortak Tez Danışmanı: Doç. Dr. Göknur Büke

Aralık 2019, 88 sayfa

Grafen karbonun bir atom kalınlığına ve petek kafes yapısına sahip allotropudur. Grafen birçok olağanüstü özelliğe sahiptir ve bu özellikler ona duyulan ilginin de artmasına sebep olmuştur. Grafen bilinen en iyi elektrik iletkenliğine sahip malzemedir. Ayrıca yüksek birim yüzey alanı, yüksek saydamlık, yüksek dayanç gibi özellikleri de grafeni bir çok uygulama için uygun bir aday haline getirmektedir. Grafenin icadından beri, grafenin nasıl üretileceği ve nasıl verimli bir şekilde kullanılacağı üzerine bir çok araştırma yapıldı ancak grafenin büyük miktarlarda üretilmesi hala mümkün değildir. Bu nedenle de grafenin fiyatı oldukça yüksektir ve özel uygulamalar dışında kullanımı kısıtlıdır.

Bu çalışmada, grafen, grafitin elektrokimyasal yapraklanması ile sentezlendi. Bu yöntem, grafeni yüksek üretim hızında ve kaliteli olarak elde etmek için en uygun maliyetli yöntem. Bu metotta, elektrolitik hücredeki elektrodlar (bir tanesi veya ikisi de grafit) arasında potansiyel fark uygulanır ve grafen levhaları grafit elektrottan koparılır. Bu çalışmada, yüksek kaliteli grafeni yüksek üretim hızında elde etmek için uygulanan potansiyel, kullanılan elektrodlar ve elektrolitler ve hücre geometrisi

gibi deęişkenler optimize edilmiştir. Sentezlenen grafen SEM, EDS, TEM, XRD, AFM, BET, FTIR ve Raman spectroscopyi kullanılarak karakterize edildi.

Anahtar Kelimeler: Grafen, elektrokimyasal yapraklanma, elektrolit, karakterizasyon

Dedicated to my family

## ACKNOWLEDGEMENTS

First of all, I would like to thank my supervisor, Prof. Dr. M. Kadri Aydınol for his patience, encouragement, advisement and sharing his knowledge and experience without stinting. He has extended continuous support, encouragement, and constant guidance throughout my entire graduate research. I am very grateful for the freedom he provided me in conducting research. Also, I want to express my gratitude to my co-supervisor, Assoc. Prof. Dr. Göknur Büke for her guidance. Her comments, suggestions and discussions was very valuable for me.

I want to thank to my friends at the Department of Metallurgical and Materials Engineering, METU for their support and sharing their knowledge and experience without stinting, especially Burcu Arslan, Özgün Köse, Cansu Savaş Uygur and Alp Yıldırım. Furthermore, I would like to thank to Serkan Yılmaz for SEM trainings and analysis, and Nilüfer Özel for her supports to XRD analysis.

Moreover, the supports of my friends Mehmet Can Zaybek, Dilek Sezer, H. Merve Ertuğrul, Burhan Can Yiğit and Murat İlerigelen is memorable for me since we were undergraduate students. Their companionship always made me happy. Special thanks to Aşina Pamuk for reading and editing my thesis. Also, I want to thank Eren Erol for his support to my thesis.

I also want to thank to my colleagues and friends at TAI and ODTÜ-WTNDT for their supports.

I would like to express my sincere thanks to my parents, Süleyman and Suna Kurt for their endless love, patience and supports throughout my life. I am also grateful to my sisters, Gülsün, Esin and brother, Yasin for their continuous support and encouragement.

## TABLE OF CONTENTS

ABSTRACT .....	v
ÖZ .....	vii
ACKNOWLEDGEMENTS .....	x
TABLE OF CONTENTS .....	xi
LIST OF TABLES .....	xv
LIST OF FIGURES .....	xvi
1. INTRODUCTION .....	1
1.1. What is Graphene? .....	1
1.1.1. Objective of The Study .....	4
2. LITERATURE REVIEW .....	7
2.1. Properties of Graphene .....	7
2.1.1. Electrical Properties of Graphene .....	7
2.1.2. Mechanical Properties of Graphene.....	10
2.1.3. Other Properties .....	11
2.2. Usage areas of Graphene .....	11
2.2.1. Electrical Applications.....	11
2.2.2. Batteries and Capacitors .....	13
2.2.3. Optical Electronics.....	15
2.2.4. Graphene Based Composite Materials.....	16
2.2.5. Anti-corrosive Applications and Painting.....	17
2.2.6. Membranes and Filters.....	17
2.3. Production Methods of Graphene.....	18

2.3.1. Bottom Up Methods .....	19
2.3.1.1. CVD (Chemical Vapor Deposition) .....	19
2.3.1.2. Epitaxial Growth.....	19
2.3.2. Top Down Methods.....	22
2.3.2.1. Micromechanical Cleavage .....	22
2.3.2.2. Hummers Method .....	23
2.3.2.3. Liquid Phase Exfoliation .....	24
2.3.2.4. Mechanical Milling of Graphite .....	25
2.3.2.5. Electrochemical Exfoliation of Graphite .....	26
2.4. Characterization Methods .....	35
2.4.1. Raman Spectroscopy .....	35
2.4.2. X-Ray Analysis .....	37
2.5. BET (Branauer-Emmett-Teller) Analysis.....	38
2.6. FTIR.....	38
3. MATERIALS AND METHODS .....	41
3.1. Materials.....	41
3.1.1. Graphite Rods.....	41
3.1.2. Chemicals .....	42
3.1.2.1. Exfoliation Agents .....	42
3.1.2.2. Antioxidant Agents .....	43
3.1.2.3. Surfactants .....	43
3.1.2.4. Catalyzer .....	43
3.2. Experimental Setup .....	44
3.3. Materials Characterization Methods .....	46

3.3.1. SEM .....	46
3.3.2. TEM .....	46
3.3.3. X-Ray .....	46
3.3.4. BET (Branauer-Emmett-Teller).....	46
3.3.5. Raman Spectroscopy.....	46
3.3.6. FTIR Analysis.....	47
4. RESULTS, CHARACTERIZATION AND DISCUSSIONS .....	49
4.1. Parameters of Experiments.....	49
4.2. Studies on the Filtered Particles .....	51
4.3. Effects of Exfoliation Agent and Antioxidants .....	53
4.3.1. Experiments with NaOH.....	54
4.3.2. Experiments with H <sub>2</sub> SO <sub>4</sub> .....	55
4.3.2.1. With Antioxidant Agent NaOH .....	55
4.3.2.2. With Antioxidant Agent LiOH .....	56
4.3.2.3. With Antioxidant Agent KOH and NH <sub>4</sub> OH.....	57
4.3.3. Experiments with HNO <sub>3</sub> .....	58
4.3.4. Experiments with H <sub>2</sub> SO <sub>4</sub> / HNO <sub>3</sub> .....	58
4.3.4.1. The Effect of Current .....	58
4.3.4.2. The Effect of the molarity of Exfoliation Agent.....	62
4.3.4.3. With No Antioxidant Agent.....	68
4.3.4.4. With Antioxidant Agent KOH .....	70
4.3.4.5. With Antioxidant Agent NH <sub>4</sub> OH.....	73
4.3.4.6. With Antioxidant Agent NaOH .....	75
4.3.5. Other Characterizations .....	75

5. CONCLUSIONS .....	77
5.1. Conclusions.....	77
5.2. Recommendation for Future Work .....	78
REFERENCES .....	79

## LIST OF TABLES

### TABLES

Table 2.1. Properties of graphene [4,5].	7
Table 2.2. Electrical Properties of Graphene.	9
Table 2.3. Mechanical Properties of Graphene.	10
Table 3.1. Chemicals used in this study.	42
Table 4.1. Experiments	50
Table 4.2. EDS results of the experiments.	54
Table 4.3. Effect of exfoliation agent on E.R.	62

## LIST OF FIGURES

### FIGURES

Figure 1.1. Graphene structure [2].....	2
Figure 1.2. Graphene sheets in graphite structure [2].....	2
Figure 1.3. A schematic of ‘bottom-up’ and ‘top-down’ graphene synthesis [3].....	3
Figure 1.4. Quality vs Cost Sketch of Graphene Synthesis Methods.....	5
Figure 2.1. Structure and morphology of graphene: (A) Corrugated graphene (B) Zigzag edge graphene and armchair edge graphene.....	9
Figure 2.2. Flexible-transparent electronics with graphene [26].....	12
Figure 2.3. Schematic diagram of graphene-based supercapacitor device [87]. .....	15
Figure 2.4. Graphene membranes [40]. .....	18
Figure 2.5. Fundamental processes during epitaxy [49].....	21
Figure 2.6. Schematic of experimental cell, electrochemical intercalation and exfoliation process. ....	27
Figure 2.7. The growth rate of GNs as an increasing function of exfoliation temperature: (a) CV and (b) CC model. The Arrhenius plots of $\ln RGN$ versus $1/T$ under (c) CV and (d) CC model. ....	33
Figure 2.8. Raman spectrum of (a) graphite and (b) exfoliated AFLG, indicating high-quality, few-layer graphene.....	36
Figure 2.9. Raman Spectrum of Pristine Single Layer Graphene.....	37
Figure 2.10. XRD spectrum of graphite, graphene oxide and graphene nano sheets [91].....	38
Figure 2.11. <i>FTIR spectrum of graphene oxide and graphene [90]</i> .....	39
Figure 3.1. XRD spectrum of graphite rod. ....	41
Figure 3.2. Experimental Setup .....	44
Figure 4.1. SEM images of region 1, 2 and 3 from experiment 10. ....	51
Figure 4.2. SEM images of filtered particles .....	51

Figure 4.3. SEM images of experiment 10 .....	52
Figure 4.4. Thickness measurements of particles with AFM.....	53
Figure 4.5. (a) The SEM image of particles), (b) XRD Spectrum of particles with 1.5M NaOH (exp 1.....	55
Figure 4.6. The SEM images of particles with (a) 0.25M H <sub>2</sub> SO <sub>4</sub> with 5.5V and 0.5A (exp 2, (b) 0.25M H <sub>2</sub> SO <sub>4</sub> with 5.5V and 0.35A (exp. 3).....	56
Figure 4.7. (a)The SEM images, (b) XRD spectrum of graphene particles with 0.25M H <sub>2</sub> SO <sub>4</sub> with 5.5V and 0.2A (exp. 4).....	56
Figure 4.8. The SEM images of particles with 0.3M H <sub>2</sub> SO <sub>4</sub> with 3V and 0.3A (exp 6). .....	57
Figure 4.9. The SEM images of graphene particles with in edge region and XRD spectrum of particles , 0.3M H <sub>2</sub> SO <sub>4</sub> with 3V and 0.3A (exp. 6).....	57
Figure 4.10. The SEM images and XRD spectrum of particles with HNO <sub>3</sub> were used as exfoliation agent (exp 8). .....	58
Figure 4.11. SEM images of the powders obtained with current 0.55A, 0.27A and 0.15A.....	59
Figure 4.12. XRD spectrum of As-Received Graphite Rod, Experiments 11,12 and 14.....	59
Figure 4.13. Current effect on quality of the powders .....	61
Figure 4.14. Percentages of floating, suspended and settled powders. ....	62
Figure 4.15. SEM images of Region 2 a-c) Experiment 13, d-f) Experiment 14 .....	63
Figure 4.16. SEM and Raman Spectroscopy results of region 1 of the experiment 14. ....	64
Figure 4.17. The SEM images of graphene particles with 0.25M H <sub>2</sub> SO <sub>4</sub> , 0.4M HNO <sub>3</sub> , 5.5V and 0.15A (exp. 14).....	64
Figure 4.18. The SEM images of graphene particles with 0.25M H <sub>2</sub> SO <sub>4</sub> , 0.4M HNO <sub>3</sub> , 5.5V and 0.15A (exp. 14).....	65
Figure 4.19. XRD Spectrum of Experiment 14 and Experiment 13. ....	66
Figure 4.20. BET analysis of experiment 13 and14.....	67
Figure 4.21. FTIR spectrum of the experiment 13, experiment 14.....	68

Figure 4.22. The SEM images of particles with 1M H <sub>2</sub> SO <sub>4</sub> and 0.6M HNO <sub>3</sub> were utilized together with 2.5V and 0.3A (exp. 9). .....	69
Figure 4.23. XRD Spectrum of GO Peak in Experiment 9. ....	70
Figure 4.24. The SEM image and XRD spectrum of particles with 0.25M H <sub>2</sub> SO <sub>4</sub> and 0.4M HNO <sub>3</sub> with 4V and 0.2A (experiment 15).....	71
Figure 4.25. The SEM images of graphene particles with 0.2M H <sub>2</sub> SO <sub>4</sub> and 0.3M HNO <sub>3</sub> with 3V and 0.5A (exp. 10). ....	72
Figure 4.26. The TEM images of graphene sheets for experiment 10. ....	72
Figure 4.27. Graphene layers in TEM image for experiment 10.....	73
Figure 4.28. The SEM images of graphene particles with 0.25M H <sub>2</sub> SO <sub>4</sub> , 0.4M HNO <sub>3</sub> , 0.2M NH <sub>4</sub> OH with 4V and 0.2A (exp16).....	74
Figure 4.29. XRD spectrum of experiment 16 .....	74
Figure 4.30. BET analysis of experiment 4, 7, 13 and14. ....	75





## CHAPTER 1

### INTRODUCTION

#### 1.1. What is Graphene?

Graphene is a one layer of aromatic structure, two dimensional planar sheet of  $sp^2$  bonded carbon atoms. It could be also described as composed of benzene rings stripped out from their hydrogen atoms [1]. The carbon-carbon bond ( $sp^2$ ) length in graphene is approximately 0.142 nm. Furthermore, interlayer spacing distance of graphite is 0.335 nm [2]. Figure 1.1 and 1.2 show graphene structure. Since its discovery by Andre Geim and Kostya Novoselov in 2004, graphene has received huge attention due to its remarkable and unique features. Graphene has a large specific surface area ( $2630 \text{ m}^2/\text{gr}$ ), high Young's modulus (approximately 1 TPa), high intrinsic charge mobility ( $200000 \text{ cm}^2/\text{V.s}$ ), high thermal conductivity ( $5000 \text{ W/m.K}$ ), significant optical transmittance (97.7 %) and it conducts electricity in the limit of no electrons. Graphene is an excellent candidate for several applications such as transparent conductive electrodes, batteries, super capacitors, graphene based electronics, fuel cells, solar cells, membranes, transistors, biosensors, molecular gas sensors and composite materials.

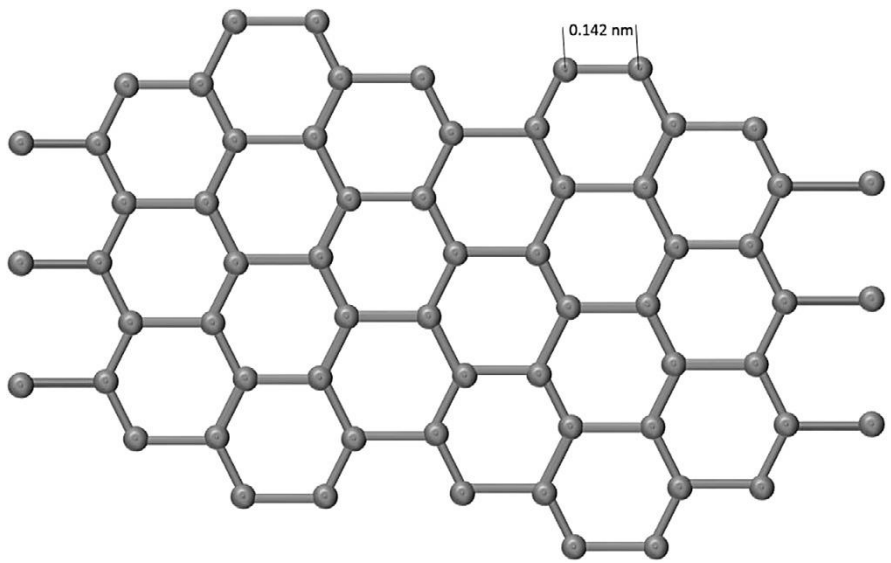


Figure 1.1. Graphene structure [2]

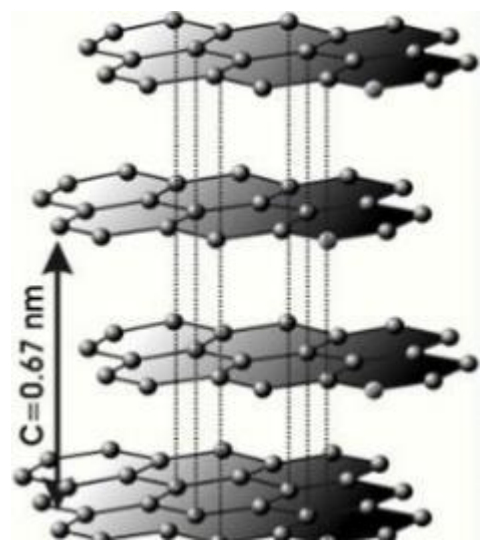


Figure 1.2. Graphene sheets in graphite structure [2].

There are many methods to synthesize graphene. These methods can be divided as top down methods and bottom up methods (figure 1.3.). Graphene was discovered by one of the top down methods which is micromechanical cleavage. Other basic top down methods are Hummers method, Tour method, chemical and thermal reduction

of graphene oxide, sonochemical liquid phase exfoliation, microwave and electrochemical exfoliation of graphite. CVD (chemical vapor deposition) and SiC thermal decomposition are the main bottom up methods.

Graphite is an abundant material that is used in top down methods; and main difficulty is to overcome the strong cohesive energy of the  $\pi$  layers in graphite (5.9 kJ / mol carbon) [3]. Produced graphene generally consists of monolayers, bilayers and multilayers (these multilayers could be accepted as graphene upto 10 layers) and they have generally irregular structures like flakes. These flakes are flat or folded sheets and are suitable materials in the energy storage and energy conversion applications.

The main objective of scientists is to produce defect free graphene which has few layers. In top down methods, it is difficult to synthesize graphene as large pieces and few layers. The main application area of these large pieces is in electronic devices. For that kind of applications, graphene that is produced by bottom up techniques may be more useful. In bottom up techniques, basically, single layers of graphene are grown up on a substrate. Main bottom up techniques are epitaxial growth of graphene on a substrate by chemical vapor deposition (CVD), pyrolysis, solvothermal synthesis, and thermal decomposition of silicon carbide (SiC) wafer under ultrahigh vacuum conditions. Graphene is difficult to obtain free from substrate since it is nearly impossible to grow without using a substrate to support graphene.



*Figure 1.3. A schematic of 'bottom-up' and 'top-down' graphene synthesis [3].*

### **1.1.1. Objective of The Study**

The aim of the study is investigation and optimization of the process parameters of electrochemical exfoliation method for high yield and high quality graphene synthesis for composites, paints, filters, batteries and super capacitors.

These parameters are:

- Exfoliation agents: concentrations and types
- Current and current density
- Electrical Potential (Voltage)
- Catalyzer effect
- Antioxidant agents
- Surfactants

Graphene is one of the most promising materials in today's and future's technology. However, to produce high quality graphene on a large scale at low cost is one of the biggest obstacles in commercializing graphene. Another challenge is the reproducibility. Electrochemical exfoliation method is a convenient way to synthesize graphene for high yielding and good properties for several applications.

Quality versus cost sketch of the main graphene synthesize methods is given below. Parameters like structural disorder, defect density, and intrinsic conductivity is taken to measure the quality of graphene. In Figure 1.4, it is shown that the graphene which is synthesized by electrochemical methods have several application areas like energy storage, composites, coatings, transparent conductive layers etc.

In electrochemical exfoliation method, an ionic conductive solution (electrolyte) and direct current (DC) are used to make structural changes into graphite upon ionic intercalation. Graphite rod, plate or wire could be used as electrode.

As mentioned before, the main objective of this study is to determine optimal parameters for the electrochemical exfoliation process. One of them is the choice of the electrolyte. The important factors that electrolyte must have are high ionic conductivity, electrochemical stability and non-flammability. It should also allow fine-tuning of the electrochemical variables.

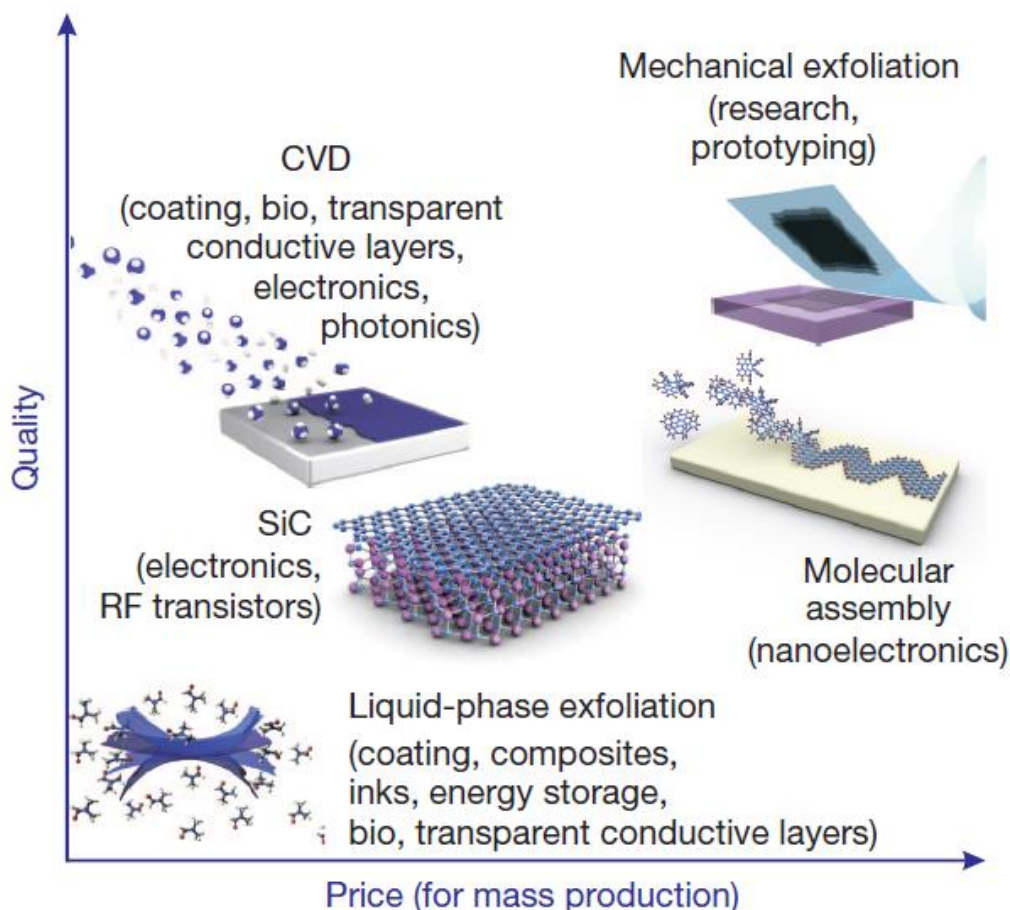


Figure 1.4. Quality vs Cost Sketch of Graphene Synthesis Methods

Novoselov et al., A roadmap for graphene, Nature 490, 192-200, 2012.

Applied voltage and current are significant parameters, too. Applied current has important role on number of layers of graphene. The effect of these and several other parameters were investigated by analyzing the obtained product.



## CHAPTER 2

### LITERATURE REVIEW

#### 2.1. Properties of Graphene

Many researchers study on mass production, characterization and applications of graphene. Graphene has many extraordinary properties. Some of these properties are given in table 2.1.

Table 2.1. *Properties of graphene [4,5].*

Property	Details
Optical transparency	97.7 %
Electron mobility	200,000 cm <sup>2</sup> V <sup>-1</sup> s <sup>-1</sup>
Thermal conductivity	5000 Wm <sup>-1</sup> K <sup>-1</sup>
Specific surface area	2630 m <sup>2</sup> g <sup>-1</sup>
Breaking strength	42 N m <sup>-1</sup>
Elastic modulus	0.25 TPa

##### 2.1.1. Electrical Properties of Graphene

Carbon atoms have 6 electrons in total; 2 of them are inner shell electrons and 4 of them are outer shell electrons. These 4 outer shell electrons are suitable to make chemical bond in singular carbon atom. On the other hand, each atom makes bond with 3 other carbon atoms on the two dimensional plane in graphene. At that situation, 1 electron is free and available to conduct electricity. These electrons have

high mobility; they are called as pi ( $\pi$ ) electrons and they are located below and above graphene sheet. These pi electrons' orbitals overlap and they help to improve carbon-carbon bonds. Basically bonding and anti-bonding of pi orbitals, the valence and conduction bands determine the electronic properties of graphene [6].

The bond length between  $sp^2$  hybridized two carbon atoms is 0.142 nm and interplanar distance is 0.335 nm when sheets are attached upon each other. That  $sp^2$  hybridization occur between s-orbital and two p-orbitals and it results trigonal planar structure [7].

The magnetic properties and electronic properties of graphene are determined by edge of graphene. Zigzag edge graphene shows the half metallic properties with zero band gap. In addition, their magnetic properties are dominated by the external in-plane homogeneous electric field across their zigzag edges. On the other hand, armchair edge graphene can show both metal or semi-conductor nature. Armchair graphene has narrow energy band with small band gap. Structure of zigzag edge and armchair edge graphene is given in figure 2.1.

Carbon has high flexibility of bonding and so carbon based systems exhibit infinite number of different structures. The flexibility and dimensionality of these structures also result various physical properties. The sigma ( $\sigma$ ) bonds provide robustness to all allotropes of carbon. Each pi ( $\pi$ ) orbitals have one extra electron and so pi ( $\pi$ ) bands are half-filled. The half-filled  $p_z$  orbital, ( $\pi$ ) bond, perpendicular to lattice, provides electrical conductivity to graphene and it is responsible from the interaction between graphene layers and substrate [8]. Graphene has charge carriers that behave as massless, relativistic particles. Graphene is a semiconductor which has zero bandgap. Graphene has ambipolar electric field and ballistic transport over sub-micron distances at room temperature. Graphene's ballistic transport is observed as  $2 \times 10^5 \text{ cm}^2/(\text{Vs})$  at an electron densities of  $\sim 2 \times 10^{11} \text{ cm}^{-2}$ . Its charge carrier mobility is approximately  $15000 \text{ cm}^2/(\text{Vs})$ . [8,9,10]. All these properties make graphene a

suitable candidate for electronic devices. Both electron mobility and charge density control the conductivity.

When comparing with copper, graphene has higher electron mobility but lower charge density. In general, electrical properties of graphene were given in Table 2.2 [11].

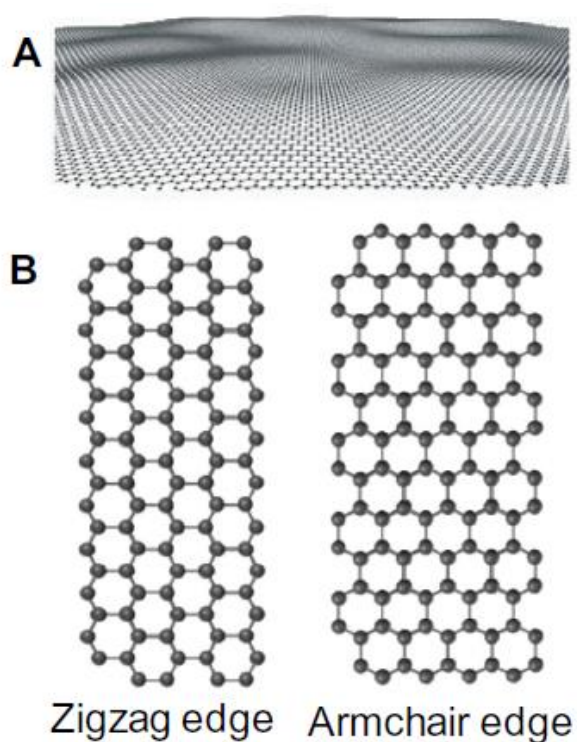


Figure 2.1. Structure and morphology of graphene: (A) Corrugated graphene (B) Zigzag edge graphene and armchair edge graphene.

Table 2.2. Electrical Properties of Graphene.

Band gap (in sheet graphene)	0 eV
Band gap (in graphene ribbons)	~3.8 eV
Electron mobility (intrinsic limit)	~200,000 $\text{cm}^2 \cdot \text{V}^{-1} \cdot \text{s}^{-1}$
Electron mobility (on $\text{SiO}_2$ substrate)	~40,000 $\text{cm}^2 \cdot \text{V}^{-1} \cdot \text{s}^{-1}$

Carrier density	$10^{12} \text{ cm}^{-2}$
Free path for electron-acoustic phonon scattering	$>2 \text{ } \mu\text{m}$

### 2.1.2. Mechanical Properties of Graphene

Graphene has some excellent mechanical properties. The mechanical properties may be seen below [11].

Table 2.3. *Mechanical Properties of Graphene.*

Tensile strength	130 GPa
Young's modulus	1 TPa
Tension rigidity	340 GPa·nm
Surface tension	54.8 mN/m <sup>8</sup>
Flexural rigidity	3.18 GPa·nm <sup>3</sup>
Thermal conductivity (freely suspended graphene)	2-4 kW·m <sup>-1</sup> K <sup>-1</sup>
Distance between adjacent layers of graphene in graphite	3.4 Å

Mechanical properties of graphene are affected by a lot of factors such as defects in graphene, tilt boundary angle and adjacent boundaries' stitching quality. [12] Firstly, the spring constant of few layer graphene (<5 layer) is measured with force displacement of AFM (atomic force microscope) in 2007. The spring constant was calculated in range of 1-5 N/m and Young's Modulus was estimated as 1 TPa. Young's Modules of graphene was calculated as 1 TPa by using AFM tip indentation until it ruptured and Young's Modules is determined from the force-depth curve [13]. Robustness in-plane of sp<sup>2</sup> bond is responsible from the such a superior property and it makes graphene strongest material which is known. Using Raman spectroscopy, similar Young' Modules of graphene was calculated later.

### **2.1.3. Other Properties**

Graphene is a superior heat conductor because of the strong bonding of its carbon atoms. Its thermal conductivity was measured between 3000 – 5000 W / (m. K) from Raman Spectroscopy and it decreases with increasing the number of layers of graphene. Because of its high thermal conductivity, graphene spread heat efficiently [14].

The optical properties of graphene are determined by direct interband electron transitions [15]. Graphene has high transmittance, it absorbs 2.3% of the light and it has negligible reflectance. (<0.1%) [16]. The white light transmission of the graphene is 97.7 % [17].

In addition, perhaps the most important property of graphene is its high specific surface area; it is calculated as 2630 m<sup>2</sup>/g theoretically. The specific surface area of graphene is derived in the range of 270-1550 m<sup>2</sup>/g experimentally [18].

## **2.2. Usage areas of Graphene**

Graphene's excellent properties like high electrical and thermal conductivity, high strength, stiffness, elasticity and high specific surface area make it suitable candidate for many applications.

### **2.2.1. Electrical Applications**

There are a lot of studies on how to utilize graphene in specific applications. Graphene is a suitable material for molecular-scale electronics. In addition, graphene

can work out as semiconductor layer in barristor, field effect transistor, as well as integrated circuits when the type and density of the carrier in the graphene p-n junction is customized [19,20,21]. Graphene can also be used to produce capacitors, sensors and electronic lenses [22].

One of the electrical application of graphene is transistors. Graphene is used in barristor which is a triode device with a gate controlled Schottky barrier and it has  $10^5$  on-off ratio. This transistor has high performance because of short gate length, and its performance does not change much with temperature and it is relatively stable [23].

In addition to electronic devices, graphene is a convenient material for photonics and optoelectronics which requires the combination of electronic and optical properties [24]. Graphene is used in optoelectronic applications as transparent conductor because of it has high transparency and low sheet resistance. Graphene can be used in solar cells as transparent conducting films as well. Graphene is a convenient candidate for flexible devices [25]. There are a lot of studies to replace ITO (Indium Doped Thin Oxide) with graphene in touch screens and light emitting devices. Usage of graphene on screens can be seen in figure 2.2 [26].

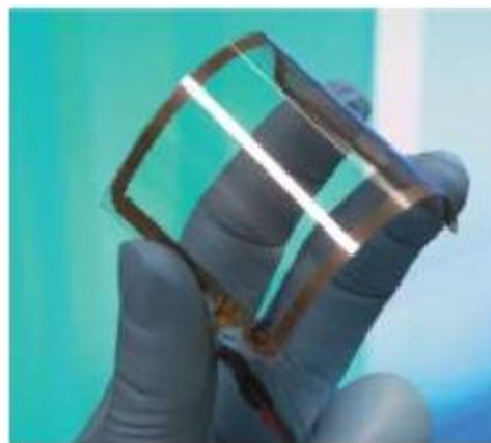


*Figure 2.2. Flexible-transparent electronics with graphene [26].*

Graphene has high specific surface area and fine electrical and mechanical properties. Graphene electrode could be used in electrochemical capacitors and these capacitors have high power density as well as high energy density and great cycle stability [27]. Vertically oriented graphene nanosheets are used in double-layer capacitors (DLCs) and these capacitors have low electronic resistance, fine resistor-capacitor time constants, and superior AC line-filtering performance. Graphene nanosheets provide more exposed edge planes and so charge storage of the capacitor increases [28].

The high quality graphene is a superior conductor and it does not have a band gap. This is the only problem with graphene because it cannot be switched off. Thus, a band gap must be constituted into graphene to use it in the future nano-electronic devices and applications [28].

### **2.2.2. Batteries and Capacitors**

Graphene can provide higher energy storage capability for especially portable electronics and electric vehicles. Graphene can be used in a lot of applications for energy storage such as high capacity and fast charging devices, smaller capacitors, transparent batteries, flexible and even rollable energy storage devices. Especially, graphene is a promising material for supercapacitors because it has extraordinary specific surface area ( $2630 \text{ m}^2/\text{g}$ ). The intrinsic capacitance was reported to be approximately  $21 \text{ }\mu\text{F}/\text{cm}^2$  for single layer graphene. For electrical double layer (EDL) capacitance, this value is accepted as an upper limit and graphene based supercapacitor's EDL capacitance can reach up to  $550 \text{ F}/\text{g}$  if the entire surface area can be used [29].

Due to graphene's high specific surface area, it is tried to substitute activated carbon in supercapacitors. High surface area is very important for capacitance and it gives

better electrostatic charge storage. Graphene based supercapacitors can store energy almost equal as lithium-ion batteries. In addition, their charging cycles may reach tens of thousands. High porous form of graphene should be utilized in order to achieve higher capacitance and faster charge-discharge.

In addition, graphene could present wide range of batteries as redox-flow batteries, lithium-sulfur batteries, metal-air batteries and most importantly lithium-ion batteries (LIBs). In both sides of graphene, the lithium ions can be stored as forming  $C_3Li$  [30]. Graphene's theoretical capacity was calculated as 744 mAh/g. On the other hand, in graphene electrodes, chemically modified and defective forms of graphene were used and so graphene electrodes capacity changing between 100 mAh/g and 1000 mAh/g. That capacity is changing with properties of graphene, electrode processing, mass loading, structural defects and surface area [31].

For lithium ion batteries, graphite is a suitable anode material, however it cannot be used in  $Na^+$  and  $Al^{3+}$  batteries because these atoms not be able to intercalate efficiently in graphite; so porous graphene composites may be an alternative for these kind of applications.

Films and bulk structures are not very useful for wearable electronics, but graphene fibers can be shaped into fabrics and textiles and so they are appropriate to construct flexible and wearable supercapacitors [32]. Application of graphene for supercapacitors can be seen in figure 2.3 schematicly.

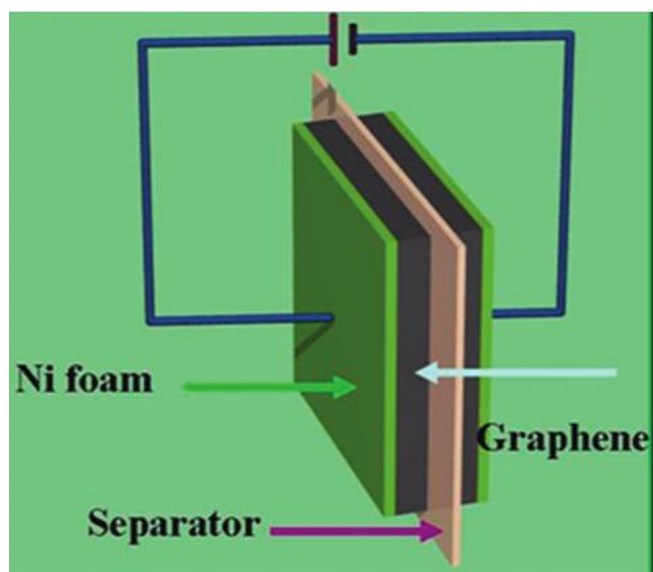


Figure 2.3. Schematic diagram of graphene-based supercapacitor device [87].

Assembling graphene sheets into 3D structure is one of the most effective ways to utilize graphene's extraordinary properties. Graphene's 2D structure provide fast electron transfer in 3D, and also its surface area is convenient and accessible for absorption and desorption of ions.

There are a lot of coating techniques to process graphene dispersion into electrodes. These techniques are mainly blade coating, electrodeposition, dip coating, spin coating, electrospinning, rod coating, spray coating, screen printing, inkjet printing, layer by layer assembly, gravure printing, electrospinning, vacuum filtration, interfacial deposition, drop casting and Langmuir-Blodgett deposition [33,34].

### 2.2.3. Optical Electronics

Studies and researches continue to use graphene in optoelectronics such as liquid crystal displays (LCD) and organic light emitting diodes (OLEDs), touchscreens. The material which is used in optoelectronic applications must have higher transmittance than 90% and also it must have at least  $1 \times 10^6 \Omega^{-1} \text{ m}^{-1}$  electrical

conductivity and so low electrical resistance. Graphene transmits light up to 97.7% and it is almost transparent.

Currently ITO (Indium Doped Thin Oxide) is the most widely used material in optical electronics. Graphene is one of the potential candidate that can be exchanged with ITO in these applications. In addition, some research show that the optical absorption of graphene can be improved by arrangement of the Fermi level. High quality graphene has very high strength and flexibility thus it is a perfect material for flexible electronic devices and screens [35].

#### **2.2.4. Graphene Based Composite Materials**

Graphene's excellent properties could be utilized in composite materials. While manufacturing these composite materials, graphene sheets must be located in composite structure at a sufficient amount. Also, they must be distributed homogeneously into various matrices. Because of graphene oxide sheets are hydrophilic, they can be swelled and dispersed in water [36]. The aqueous media is inconsonant with most organic polymers. Graphene sheets can only be dispersed in aqueous media due to its hydrophilicity.

Graphene-polymer nanocomposites may show electrical conductivity. These composites can be prepared by solution phase mixing of the exfoliated phenyl isocyanate-treated graphite oxide sheets with polystyrene. After that, chemical reduction must be applied. Graphene sheets are homogeneously dispersed in the polymer matrix in these composites. These composites contain approximately 2.4 volume percent (vol. %) graphene. SEM images of them show that almost entirely composite is filled with graphene sheets, although 97.6 vol.% is filled by the polymer. [37]

Graphene based composites are lighter, stronger, safer and greener. They can be used at aircraft wings to reduce weight and prevent lightning strike damage. In

addition, they may be used in sporting goods like skiing, cycling, tennis and formula one racing cars. Graphene could be used to reinforce concrete and other building materials.

#### **2.2.5. Anti-corrosive Applications and Painting**

Graphene can be used in many types of paints and coatings. Graphene coatings may show conductive, hydrophobic, chemically resistant properties. Graphene shows remarkable thermal and electrical conductivity and it may enable conductive paints. It also provides durability for coatings against cracks and scratches. Graphene's high adhesion property makes it a suitable material for high adhesion needed coating applications. Graphene's other potential coating applications are anti-rust coatings, anti-bacterial coatings, UV ray blockers, solar paints which are capable of absorbing solar energy and transmitting it, anti-fog paintings [38].

#### **2.2.6. Membranes and Filters**

Graphene is both a hydrophilic and hydrophobic material. Graphene oxide membranes are capable of forming a perfect barrier when dealing with liquids and gasses. They can effectively separate organic solvent from water and remove water from a gas mixture to an exceptional level. Helium is the hardest gas to block and they can even stop helium. Water is able to pass through membrane when the water layer is only one atom thick (the same size as graphene) [39].

Due to graphene's some useful properties including large specific area, single atomic layer structure, hydrophobic property and rich modification approaches, it is an excellent material for desalination process (separation of water and salt) and water purification. In figure 2.4, desalination process can be seen by the help of graphene membrane.

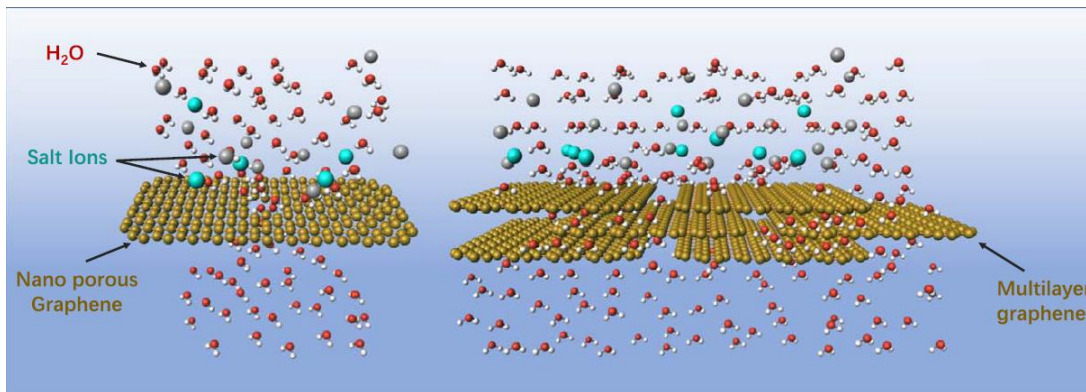


Figure 2.4. Graphene membranes [40].

Carbon based materials are one of the candidate for membrane applications because of their chemical inertness, perfect mechanical properties, environmental safety and availability of rich functional groups. Especially, graphene is widely being researched [40]. Graphene or graphene oxide membranes' structure can be modified to adjust the interlayer spacing between the layers or pore size to benefit these membranes for real applications. Graphene membranes have higher selectivity due to graphene's single atom thickness [41].

### 2.3. Production Methods of Graphene

There are a lot of methods to produce graphene. These methods can be divided as top down methods and bottom up methods.

Main bottom up methods are CVD (Chemical Vapor Deposition), Epitaxial Growth (i.e. Large single crystal graphene on Cu) and Thermal Decomposition of SiC.

Main Top down methods are:

- Mechanical Cleavage
- Hummers Method

-Liquid Phase Exfoliation

-Electrochemical Exfoliation

- \* Anodic Exfoliation

- \* Cathodic Exfoliation

### **2.3.1. Bottom Up Methods**

#### **2.3.1.1. CVD (Chemical Vapor Deposition)**

Graphene can be synthesized by CVD method both on substrate and without substrate. Low defect few layers of graphene were grown on Si substrate which is Ni film coated [42]. Generally, CH<sub>4</sub> or any other low cost carbon source from alcohol groups are used in CVD method. Density of synthesized graphene is one of the issues; increasing the growth time at synthesis temperature of 960 – 970 °C causes higher density of graphene. In addition, it is reported that higher synthesis temperature from 650 to 850 °C increases the quality of graphene grown on Cu foils. [43]. On the other hand, mass production of graphene by CVD is restricted with complex substrate preparation, i.e. using CH<sub>4</sub> gas on Cu substrates. Higher temperatures between 800 and 1050 °C result faster growth of graphene and reaction time does not affect the structure of graphene. Besides, because of the needs of high temperatures, CVD method has high energy consumption and so it is not an efficient method [44]. CVD method is researched by many researchers and the parameters still could not be optimized.

#### **2.3.1.2. Epitaxial Growth**

There are several epitaxial growth methods to synthesize graphene layers; these methods are mainly chemical vapor deposition (CVD), temperature programmed

growth (TPG), carbon feedstock, segregation based methods and SiC sublimation (thermal decomposition of SiC).

Epitaxial growth is one of the promising method for graphene synthesis. The graphene is generally grown on a hexagonal substrate in that method. Silicon carbide (SiC) is used both as the source and substrate material, so C is already present in the substrate in thermal decomposition of SiC method. In addition, close packed metals may be used as the substrate. Silicon carbide decomposes in ultra-high vacuum at elevated temperatures between 1000-1500 °C; Si is sublimated and leaves a carbon-rich surface on the substrate. The main difference between thermal decomposition of SiC and CVD is carbon is provided in a gas form in CVD and carbon is already present in substrate in thermal decomposition. Another difference is that metal is utilized as substrate to grow the graphene sheets and also catalyst in CVD [45].

Graphene is generally grown on transition metals surfaces and graphene's properties changes due to mismatch between the graphene and metal surfaces. Graphene can regulate itself at various angles with respect to the metal substrate lattice. Theoretical and experimental results of the graphene structure on the Cu (111), Cu (100), Au (111), Ni (111), Pt (111), Rh (111), Ir (111), Co (0001), Ru (0001), Re (0001) and SiC (0001) surfaces are reported by Tetlow. [45,46,47]

Defects are formed on structure during graphene growth on metals. These defects mainly formed on grain boundaries as vacancies and local imperfections of the hexagonal structure. Grain boundaries occur at different domains and different nucleation sites while graphene growth [48]. Nucleation sites unite during graphene growth and grain boundaries are formed between the crystalline domains. In addition, impurity atoms and vacancies are trapped in the structure while graphene growth and point defects occur.

Figure 2.5 shows fundamental processes during epitaxy. Firstly, hydrocarbon molecules are deposited on the surface and then they decompose via dehydrogenation reactions to form various  $C_xH_y$  species and H atoms. These new

species are able to diffuse the surface. Smaller carbon species diffuse on the surface and form small groups or aggregate into larger carbon clusters. Hydrogen atoms form  $H_2$  molecules and evaporate from the surface. Finally, C clusters attach to each other and form graphene islands [49].

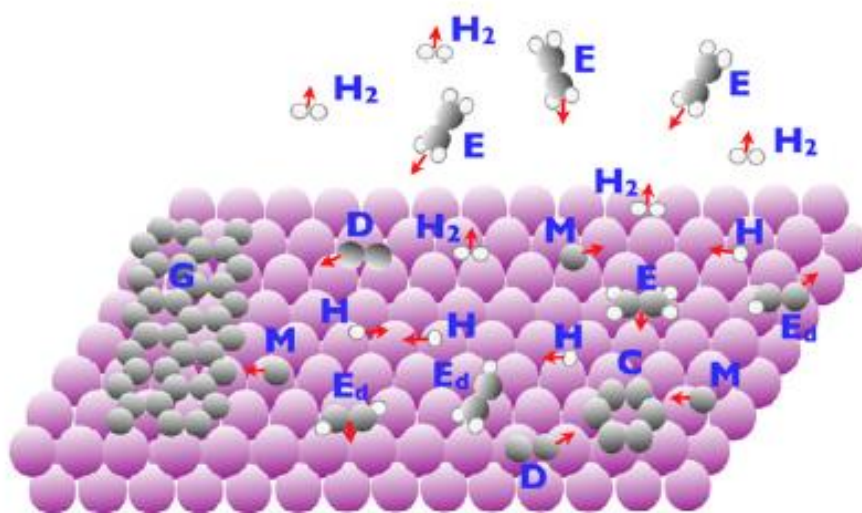


*Figure 2.5. Fundamental processes during epitaxy [49].*

Deposition method is the most controllable method in all growth processes; its deposition rate and species which are deposited may be easily determined. The process mainly consists of two steps: nucleation and growth. Nucleation may be homogeneous or heterogeneous. Graphene forms like an island on metal surfaces. In homogeneous nucleation, collision of migrating species causes to graphene islands. Stability of these island is related with temperature and concentration of the migrating species. Surface defects such as dislocations and vacancies increase the nucleation rate in heterogeneous nucleation. After graphene islands are formed, they capture migrating units and start to grow. Edge diffusion which is the movement of atoms around the edge of islands have important effect on shapes of islands. Having large surface area may result fracture of islands for some systems at low temperatures if the system cannot lower its surface energy with any rearrangement

type because of too slow migration. The deposition on the islands become significant while they become large enough as the islands grow at higher temperatures.

## **2.3.2. Top Down Methods**

### **2.3.2.1. Micromechanical Cleavage**

Micromechanical cleavage (MC) is can be referred as Scotch tape method or micromechanical exfoliation. Graphene is discovered by that method and it is also used in many fields. Among all graphene synthesis methods, micromechanical cleavage method is one of the most commonly used one. [50] This method is simple and it basically requires only a tape like scotch tape. Graphite flakes are located between adhesive tape and the surface is continuously peeled off. The cleavage of thin flakes is caused by peeling off graphite flakes and they stick to surface as cleaned. The clean tape is used to remove the flakes and few layers and even single layer graphene can be obtained with continuous process. That peeling off and replacing process can be repeated until single layer graphene is attained [51].

Geim et al. synthesized few layer graphene by using (HOPG) highly oriented pyrolytic graphite and adhesive polymer. Graphene sheets bonded tape was dissolved in acetone in order to carry graphene sheets upon the substrate. Some graphene flakes were deposited on Si wafer surface after oxidized silicon wafer being dipped in the solution. Van der Waals and capillary forces derive adherence force between oxidized Si substrate and graphene flakes. With that exfoliation technique, they synthesize few layer and single layer graphene with lateral sizes up to 10 microns [50].

The main drawback of micromechanical cleavage method is its scalability. On the other hand, synthesized graphene has high quality so that method is preferred commonly to fabricate graphene. The mechanical exfoliation method is not only

used for discovery of graphene but also it is still useful method for exploration of graphene properties and applications.

### **2.3.2.2. Hummers Method**

Hummers method is widely used because it has high scalability, good yield, low cost and it enables to disperse functionalized graphene in several solvents. This method takes place at lower temperatures and it involves less reaction time.

Hummers method include basically oxidizing graphite powders with some oxidants, like Sulphuric acid ( $H_2SO_4$ ), Potassium permanganate ( $KMnO_4$ ) and Sodium Nitrate ( $NaNO_3$ ), that generate functional oxygen groups on the graphene surface. Firstly, graphite is oxidized to graphite oxide and then it exfoliated to graphene oxide. Sulphuric acid oxidizes graphite to form graphene oxide (potassium permanganate and sulphuric acid introduce oxidizing agent to the system). These treatment destroys the  $sp^2$  bonds of graphite structure. [52] After oxidation of graphite, graphite oxide is sonicated in water and exfoliated to graphene oxide.

There are various methods to reduce graphene oxide; these methods are mainly chemical, thermal and microwave methods. Chemical methods utilize reducing agent like hydroiodic acid, amino acid, ascorbic acid, sodium borohydride, dopamine, hydrazine hydrate etc. [53,54,55]. In thermal methods, graphene oxide is reduced at high temperatures to graphene and oxygen containing groups are decomposed to  $H_2O$  and  $CO_2$  [56]. Graphene oxide can be reduced by microwave irradiation to few layer graphene [57]. Reduction step is very important for quality, physical and chemical properties and potential applications areas of produced graphene.

This method is quite favorable since it has lower cost and scalability for production. However, used chemicals such as hydrazine,  $H_2SO_4$ , sodium nitrate are toxic and dangerous in especially large volume of productions; and microwave and thermal reduction can be harmful because of high local temperatures on the surface. In

addition, functional groups that are introduced on the graphene surface inhibit some applications of graphene. Some of these functional groups can be removed from surface but produced graphene's quality is generally not enough when compared to pristine graphene. So, it is needed to find functional groups that can be easily controlled and removed. Also, this method should eliminate the use of toxic chemicals such as sodium nitrate [58].

### **2.3.2.3. Liquid Phase Exfoliation**

Graphite is exfoliated in various liquid media by favour of ultrasound or shear forces to produce graphene sheets in liquid phase exfoliation (LPE) method. The bonds that hold graphite together is weak van der Waals forces and breaking these bonds are not very difficult. Graphene's surface energy is estimated as  $46.7 \text{ mN.m}^{-1}$  by Wang et al. [59]. So, the convenient liquid medium that have similar surface energy with graphene should be used in order to minimize the interfacial tension energy between graphene sheets and solvent [60]. DMF (N,N-dimethyl formamide) and NMP (N-methyl pyrrolidone) is widely used as solvents to exfoliate and stabilize graphene.[60]

Liquid phase exfoliation method is a promising method for scalability. Basically, graphene is dispersed into a convenient solvent and it is exfoliated utilizing from ultrasonication or shear forces in LPE method. The bubbles grow and collapse during that operation and dispersed graphite exfoliate to few layer graphene. Also, pressure fluctuations result exfoliation of graphite to graphene [61].

The suitable solvents should have surface energy approximately  $40 \text{ nN.m}^{-1}$  and finding a solvent may be difficult because most of them are toxic, corrosive, quite costly and display high boiling point. There are some studies in which low boiling point solvents like ethanol, acetone, methanol and acetonitrile [62]. Water is another solvent which is used in LPE but it has to be used with modification due to its high surface tension ( $72 \text{ mN.m}^{-1}$ ). In addition, water is hydrophilic and graphene is

hydrophobic. So, some surfactants such as sodium cholate and sodium dodecyl benzenesulfonate are used with water solvent [60].

To stabilize graphene, nonionic surfactants are found to be more effective than ionic ones. Nonionic surfactants have a long hydrophilic part and a hydrophobic tail, these parts generate a steric repulsion [63].

It is quite challenging to control the flaked size of graphene in LPE. In addition, finding the suitable solvents, surfactants and liquid stabilizers may be problematic in that method. But, it is a simple and cost effective method. Also, it has a big potential for scale up to production. There are a lot of studies to optimize process parameters that can result both high concentration graphene dispersion and low amount of defects of induced graphene.

#### **2.3.2.4. Mechanical Milling of Graphite**

Mechanical milling of graphite is an alternative method to produce few layer graphene sheets. Antisari et al. synthesized graphene with high aspect ratio in distilled water for 60 hours [64]. Zhao et al. used different kind of liquid media such as anhydrous N-N-diethylformamide (DMF). They used low milling speeds in order to prevent the destruction of graphite and process takes approximately 30 hours. They tried to improve the shear force that is applied on graphite. The parameters such as diameter of milling ball, speed of the rotation, type of the used graphite, milling time, centrifugation speed and concentration of graphite in the solvent affect the quality and quantity of produced graphene [65]. They also used different organic solvents such as acetone, formamide and tetrahydrofuran (THF) in order to form stable colloidal dispersion of graphene.

Mechanical Milling of graphite method is effective and straightforward. It is a suitable method for large scale production and gives opportunity to control on process parameters. On the other hand, that method consume high energy and takes

long processing times and so it can be said that it is an expensive method. Also, defects in the final products decrease the applicability of that method [66].

### 2.3.2.5. Electrochemical Exfoliation of Graphite

Electrochemical exfoliation of graphite is a convenient way to synthesize graphene. Some carbon species like graphite rods, HOPG (High Oriented Pyrolytic Graphite), carbon papers can be used as source for electrochemical exfoliation. Mainly, graphite rods are used as electrodes and ionic liquids / water solution are used as electrolyte to synthesize functional graphene sheets with single step electrochemical exfoliation approach [67]. In addition, the electric power is used to intercalate ions into graphite and drive expansion and exfoliation of graphite. The electrical potential could be varied between -10 Volts and +10 Volts for aqueous solutions. The exfoliation process usually takes place at positive electrode. The positive electrode is exposed to oxidation and negative ions in solution intercalated into the graphite layers. Schematic of experimental cell, electrochemical intercalation and exfoliation process can be shown in figure 2.6 [79].

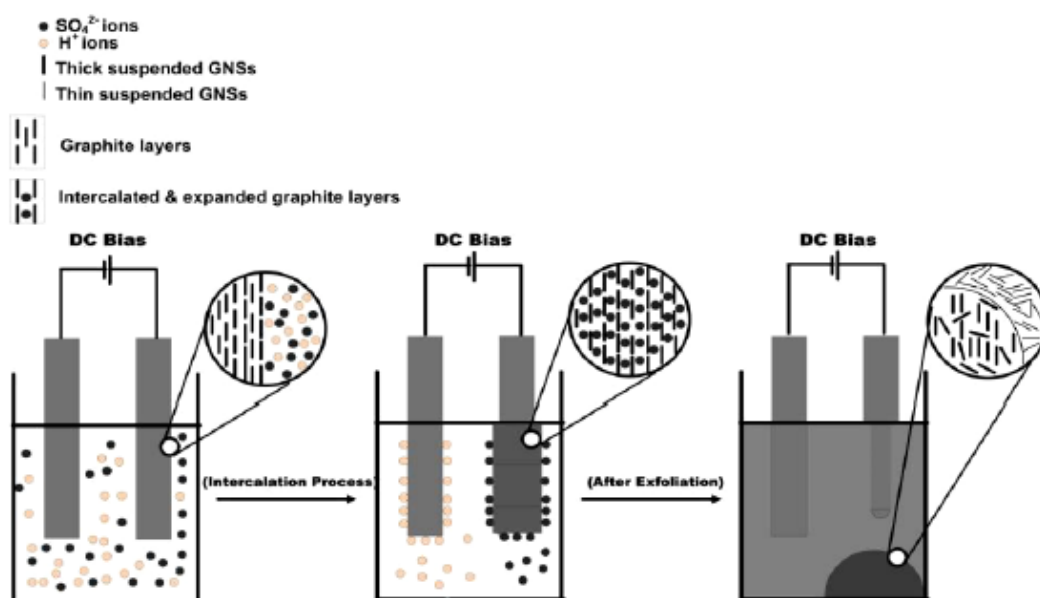


*Figure 2.6. Schematic of experimental cell, electrochemical intercalation and exfoliation process.*

The electrolyte is very important for exfoliation process and the success of the exfoliation process is based on the electrolyte. The electrolyte has two main important roles in exfoliation process:

1. The ions in electrolyte should be able to result in graphite intercalation and lead graphene sheets.
2. The electrolyte should prevent re-aggregation and agglomeration of graphene sheets. It should disperse graphene sheets efficiently.

Water is one of the most convenient candidate for electrolyte because produced suspensions are stable in water. On the other hand, electrochemical reactions in aqueous media are oxidative/anodic processes, so hydrophilicity of graphene layers may result to form oxygen containing functional groups [69].

Various type of electrolytes could be utilized such as  $\text{H}_2\text{SO}_4$  aqueous solution,  $(\text{NH}_4)_2\text{SO}_4$  aqueous solution,  $\text{LiCl}$  in propylene carbonate (PC),  $\text{LiClO}_4$  in propylene carbonate,  $\text{LiOH}$  molten salt,  $\text{LiCl}$  in dimethyl sulfoxide to synthesize few layer graphene by electrochemical exfoliation of graphite [73,74].

$\text{SO}_4^{2-}$  ions are one of the most effective ions that are used in exfoliation process. These ions have tendency to insert themselves at defective regions of edges and grain boundaries of graphite with the aid of the electrical potential [9].  $\text{SO}_4^{2-}$  ions have low reduction potential (+0.20V) and so  $\text{SO}_2$  gas can be released easily by anion depolarization. That depolarization causes the widening of interlayer distance of graphite [75]. In this method, thickness of the graphene can be controlled by regulating the electrode potential which is supplied by external power supply. The used surfactants are capable of stabilizing and holding the sheets in dispersion.

That method is generally assisted by surfactants which develop the coherence of graphene in aqueous (water based) systems. Surfactants have generally head and tail parts. Head part is polar hydrophilic and it pulls water while the hydrophobic tail

hold on the graphene surface. Thanks to these properties of surfactants, graphene may be well dispersed in aqueous solutions [71]. CTAB (Cetyl Trimethyl Ammonium Bromide), SDS (Sodium Dodecylbenzene Sulphate), SDBS (Sodium Dodecylbenzene Sulphonate) and PSS (Sodium 4-styrenesulfonate) are mainly utilized surfactants in aqueous solutions.

Liu et al published the first study on electrochemical exfoliation of graphite in 2008. They synthesized graphene by anodic exfoliation in ionic liquids. Graphene can be synthesized in film form on the various kind of substrates with that method. The author reported that electrochemical exfoliation method is suitable and promising method to synthesize graphene with high electrical conductivity and structural homogeneity. They carried out their experiment with ionic liquid and water. As an electrolyte, 10 ml water and 10 ml 1-octyl-3-methyl imidazolium hexafluorophosphate was used. They applied 15 V static potential between two graphite electrode for 6 hours at room temperature [67].

In this method, high electrical potential ( $-7/+7$ ) can be applied between two electrodes. Liu et al. [68] performed electrochemical exfoliation with constant current of 0.1A. The anions such as  $\text{SO}_4^{2-}$  are directed to positive electrode. With the removal of the electrons by the current flow, electrochemical oxidation reactions such as carboxylation, anodic oxidation and hydroxylation of graphite and water oxidation were initiated. Surface, grain boundaries and structural defect sites are main regions that these processes occur. As an electrolysis product,  $\text{O}_2$  and  $\text{CO}_2$  also can be produced during these processes.

Chien-Te Hsieh and Jen-Hao Hsueh used natural graphite (2 x 2 x 1.5 cm) as a working electrode, platinum foil (2 x 1.5 cm) as counter electrode and  $\text{H}_2\text{SO}_4$  solution as an electrolyte. They applied both CV model and CC model exfoliation at different temperatures (300, 313, 323, 333 K) [76]. They mainly studied effect of temperature on exfoliation process.

Ching Yuan Su et. al. performed electrochemical exfoliation method by using  $\text{H}_2\text{SO}_4$  solution in their experiment in 2011. They utilized 0.5 M  $\text{H}_2\text{SO}_4$  solution as electrolyte, graphite anode and platinum cathode. In their experiment, firstly +1 V was applied to the graphite for 5-10 minutes, then +10 V was applied for 1 minutes. KOH was added to electrolyte in order to reduce the oxidizing effect of  $\text{H}_2\text{SO}_4$  on graphite. Low defect graphene was obtained in the experiment but with lower yield. Author also tried to optimize the exfoliation conditions; he changed potential between +10 V and -10 V to synthesize graphene with desired amounts and properties [77].

Parvez et. al. carried out the electrochemical exfoliation experiment by using 0.1 M  $\text{H}_2\text{SO}_4$  solution as electrolyte, graphite as working electrode and platinum wires as counter electrode. They also used other inorganic salts such as ammonium chloride, ammonium sulfate, potassium sulfate, sodium nitrate and sodium chloride. They applied +10 V potential to graphite electrode for exfoliation. They claimed that sulfate ions are the most effective exfoliation performance among all. 85% of synthesized graphene was less than 3-4 layers [73].

Sanjeeva et. al. used sodium hydroxide and hydrogen peroxide ( $\text{H}_2\text{O}_2$ ) together in their experiments and they investigated that hydrogen peroxide increases yielding of exfoliation process [78].

Sumanta et. al. also carried out their experiments by using  $\text{H}_2\text{SO}_4$  solution as electrolyte. 3mm thickness pyrolytic graphite sheets were used as both working electrode and counter electrode in experiment. They focused the effect of electrolyte concentration on process and changed electrolyte concentration as 0.1M, 0.3M, 0.5M and 1M. They applied +10 V to graphite electrode firstly as a cathodic pretreatment. After that, anodic exfoliation was applied with potential increasing from 0 V to 5 V. After getting graphene in electrolyte solution, he washed them with water and applied sonication for 4 hours. After obtained homogeneously dispersed graphene colloidal, he centrifuged solution at 6000 rpm for 30 min to get

graphene powders from solution. As a result, graphene was synthesizing with lateral dimension of 11 micrometers to 26 micrometers. They reported that 4 – 6 stacked layers of graphene was synthesized. [79].

Su et. al. performed various electrolytes like HCl, HBr, HNO<sub>3</sub>, H<sub>2</sub>SO<sub>4</sub> and they reported that H<sub>2</sub>SO<sub>4</sub> is the most effective exfoliation agent for highly oriented pyrolytic graphite and natural graphite flakes. They applied 10 V to synthesize graphene.

Khanra et. al. used carboxylate ions in the electrochemical exfoliation of graphite. They prepared an electrolyte with sodium hydroxide and 9-anthracene carboxylate (ACA) to produce graphene oxide nanoparticles. They suggest that ACA ions take hold to anode (positive electrode) and were adsorbed by electrostatic interaction. After that, layers are separated from graphite anode with ACA ions. Exfoliation takes place by repeating these processes and layers were obtained with 0.79 nm thickness but also with a high (approximately 22.5%) oxygen content [80].

Wang et. al. [81] synthesize few layer graphene in propylene carbonate (PC) in cathodic process. They were inspired from electrochemical reactions between graphite anode and organic carbonates in lithium ion batteries. The organic ions or molecules enable to intercalation and expansion of graphite to graphene layers. In addition, that process needs a sonication step in order to synthesize electrode exfoliation and -15 V electrical potential should be applied. On the other hand, organic molecules were not very good for that process because they are sensitive to oxygen and moisture. In addition, the reaction rate is usually low for that process.

Solution's pH has high effect to control the kinetics of intercalation. The intercalation is very easy and strong in acidic solutions; so that a lot of expanded graphite particles may drop from graphite anode without completing their exfoliation process to graphene sheets. Graphene yielding may be not very high with strong acidic electrolytes because synthesized graphene platelets are relatively thick. These platelets consist a lot of graphene layers and graphene oxide particles but they also

consist graphene particles. So, the synthesized exfoliation products need sonication to produce high amounts of graphene sheets or flakes [69,82].

The process can take place under constant current (CC) and constant voltage (CV). When temperature fixed, exfoliation rate of graphene under constant current is approximately 5 times higher than that under constant voltage model. The CC model drive higher current density than CV model and CC model enables the advance of electrolysis of water leading to higher exfoliation rate. Chien-Te Hsieh reported that under CC in a 250 ml solution, more than 1.8 g graphene is produced in 1 hour. Activation energy is calculated from Arrhenius plots as 20.6 kJ/mol for CV and 23.1 kJ/mol for CC model exfoliation [76].

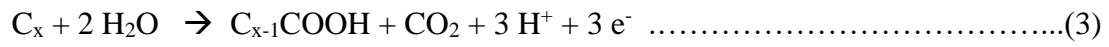
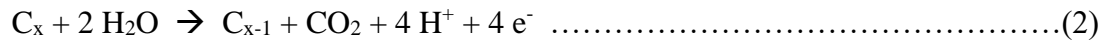
On the other hand, graphene quality may be lower at higher temperatures because higher temperatures result broken layers and fragments. High reaction rate and severe releasing of gaseous species may result in decreasing graphene quality [76].

Both constant potential (CV) and constant current (CC) models consist of 3 basic steps:

1. Surface wetting on the graphite surface and ionic adsorption
2. Intercalation of the ions by the aid of low current or low voltage
3. Edge exfoliation and in depth exfoliation of graphite at high current and high voltage

The graphene layers are mainly formed from H<sub>2</sub>O interaction with graphite. The generation of SO<sub>2</sub> and O<sub>2</sub> gases exfoliate graphite. Water is oxidized and generate OH<sup>-</sup> ions (hydroxyl) and oxygen radicals and they cause corrosion of grain boundaries, edge sites, defect sites of graphite [83]. At the same time, graphite layers (C<sub>x</sub>) react with water molecules as follows below:





The electrochemical exfoliation process is exothermic reaction; and growing rate of graphene increases with temperature. Growing rate of graphene ( $R_{GN}$ ) in CC exfoliation is 5 times higher than CV exfoliation model in between 27-60 °C [76]. In figure 2.7, growing rate of graphene is shown at different temperatures.

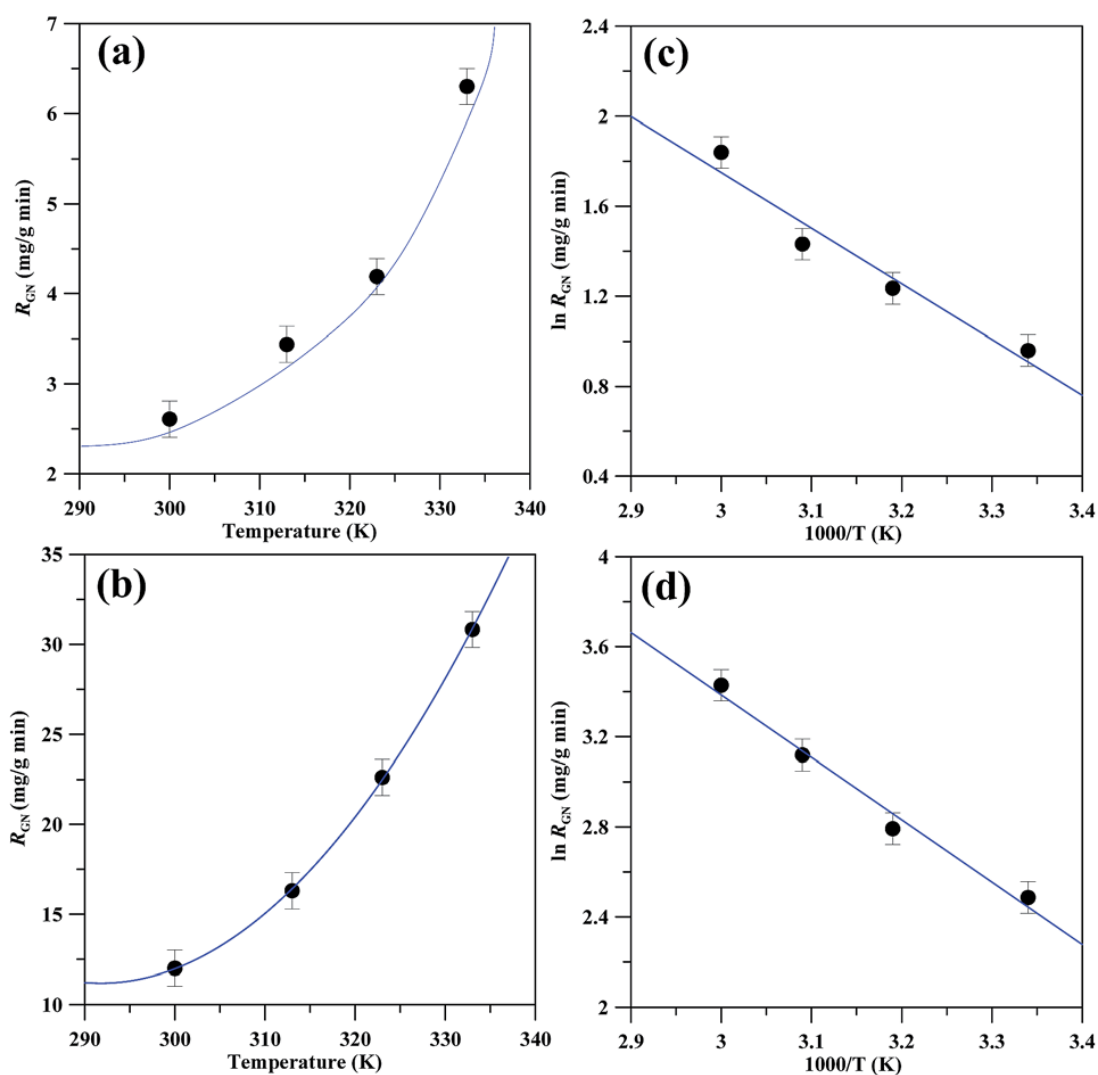


Figure 2.7. The growth rate of GNs as an increasing function of exfoliation temperature: (a) CV and (b) CC model. The Arrhenius plots of  $\ln R_{GN}$  versus  $1/T$  under (c) CV and (d) CC model.

Growing rate of graphene is shown as  $30.2 \text{ mg g}^{-1} \text{ min}^{-1}$  for CC exfoliation model and  $6.1 \text{ mg g}^{-1} \text{ min}^{-1}$  for CV exfoliation model. In the figure 2.7, Arrhenius plots were shown and  $E_{app}$  values were calculated as  $20.6 \text{ kJ mol}^{-1}$  for CV model exfoliation and  $23.1 \text{ kJ mol}^{-1}$  for CC model exfoliation. It is seen that growth rate of graphene is less related to temperature in CV model exfoliation [76].

The electrochemical exfoliation process consists of 4 main mechanisms [76]. These are:

- I) Ionic intercalation (Anodic exfoliation of water)
- II) Anion insertion and polarization (Hydroxylation or oxidation of graphite of graphite edge planes)
- III) Water electrolysis and gas evolution
- IV) Bubble expansion

In ionic intercalation step, water is oxidized at anode and form oxygen and hydroxyl radicals as according to below formula:



These ions start to oxidation and hydroxylation at grain boundaries and edge sites of graphene electrode. In anion insertion and polarization step,  $\text{SO}_4^{2-}$  ions start to insert into the graphite. Defective sites are opened up and totally are filled up by  $\text{SO}_4^{2-}$  ions and water molecules with increasing period of time. In water electrolysis and gas evolution step,  $\text{SO}_2$  and  $\text{O}_2$  gases are released with reduction of anions and oxidation of water. These reactions can be shown below:



In bubble expansion step, these gas species are propagated and cause the exfoliation of graphite to graphene layers.  $\text{SO}_2$  gas has low reduction potential (+0.20 V) and formation of  $\text{SO}_2$  is fast, so exfoliation rate is higher in the presence of  $\text{SO}_2$  [6]. Water molecules can adsorb on the graphite surface because graphite surface is hydrophilic. Electrolysis of water produce oxygen gas may assist the graphite exfoliation to graphene when DC bias is applied [76]. Intercalation occurs by ionic anions between graphite layers and the graphite-intercalation-compounds (GICs)

formed. After that, these GICs are precipitated by oxidative cleavage [70]. The process can also take place as cathodic exfoliation. Cathodic control of process is used for exfoliation in order to prevent induced surface oxidation and chemical functionalization and so that produce high quality graphene sheets.

Graphite has high electrical conductivity and high capability to store lithium between its graphene layers, so graphene has been used in lithium ion batteries as negative electrode for some time. The intercalation compounds between lithium and graphite can decompose in water easily lithium hydroxide and graphene sheets form. This process may be one of the alternative methods to produce graphene. There are some studies based on this principle, in which, they were able to produce large flakes (max 20-micron lateral dimension). They used DMSO based electrolyte which contains triethylammonium and Li ions in their experiments [69].

Although cathodic exfoliation process has some advantages, there are not many groups who study on cathodic process; and so there is limited success to synthesize graphene by totally cathodic exfoliation.

## **2.4. Characterization Methods**

There are several methods to characterize the graphene powders. These methods are basically: Raman Spectroscopy, XRD analysis, BET analysis, TEM analysis, SEM and EDS analysis, AFM analysis, FTIR analysis.

### **2.4.1. Raman Spectroscopy**

Raman spectroscopy is used to characterize  $sp^2$  and  $sp^3$  hybridized carbon atoms. It is generally used for graphite, graphene, carbon nanotubes and fullerene. Graphene species can be varied as single layer, double layer and multi-layer graphene by using Raman spectroscopy. In addition, Raman spectroscopy can be used to determine the layer number of graphene.

Figure 2.8 shows the Raman spectrum of graphite and high quality anodic few layer graphene. The ratio of D band intensity to G band intensity ( $I_D/I_G$ ) represents defect/disordered carbon structure [78].

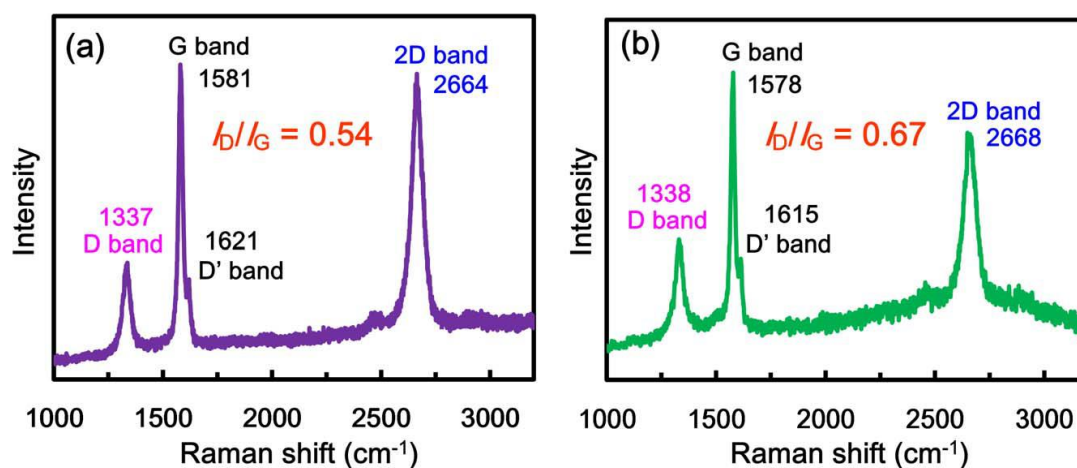


Figure 2.8. Raman spectrum of (a) graphite and (b) exfoliated AFLG, indicating high-quality, few-layer graphene.

The  $sp^2$  bonded carbon atoms are responsible from G band. G band is the result of C-C band in graphitic materials. Randomly spreaded impurities may result to split G peak into 2 peaks. G band appears close to 1580  $cm^{-1}$  and it is very sensitive to strain effects of layers. So G band is used to determine the layer number of graphene. When layer number of the graphene increases, G band moves to lower frequencies. In general, intensity ratio of G and 2D bands gives an opinion about layer number of the powders. When  $I_G / I_{2D}$  gets smaller, the layer number of the graphene becomes less.

D band shows disorder and there is no D band in perfect graphene structure (see figure 4.9).

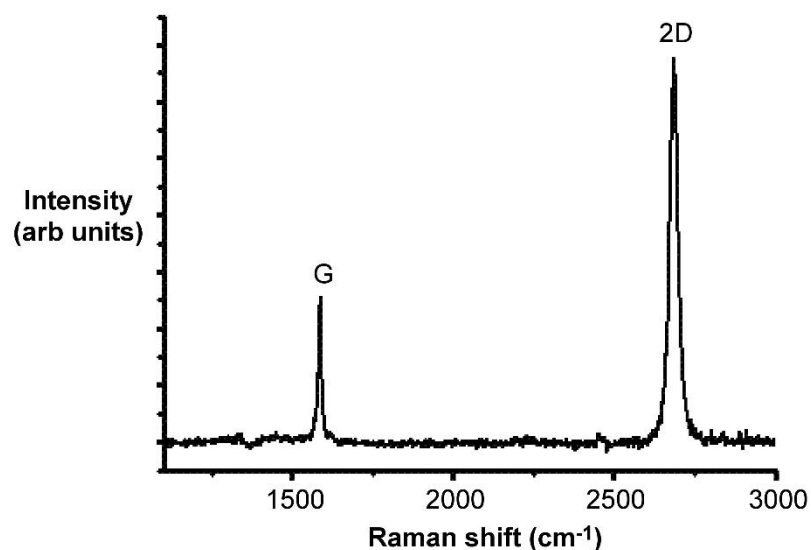


Figure 2.9. Raman Spectrum of Pristine Single Layer Graphene.

#### 2.4.2. X-Ray Analysis

XRD analysis shows the structural changes of graphitic structure which is related to the interplanar expansion. The XRD spectrum of graphite has four intensive peaks. These peaks are at  $12.9^\circ$  (001) plane,  $26.5^\circ$  (002) plane,  $42.4^\circ$  (100) plane and  $54.3^\circ$  (004) plane. Graphite's characteristic peak is one sharp and intensive peak at  $26.5^\circ$  as 8002) basal plane. In graphene, this peak becomes broad. Other peaks at  $42.4^\circ$ ,  $54.3^\circ$  which are corresponding to (100) and (004) crystal planes indicate increasing in interlayer spacing in graphitic structures. These peaks can give ideas about the presence of graphene. On the other hand, graphene oxide has a peak about  $12.98^\circ$  (001) plane. Figure 4.35 shows the theoretical XRD spectrum of graphite, graphene and graphene oxide. As seen in figure 2.10, graphene peak shifts to left and graphene oxide has one peak between  $10^\circ$  and  $15^\circ$ .

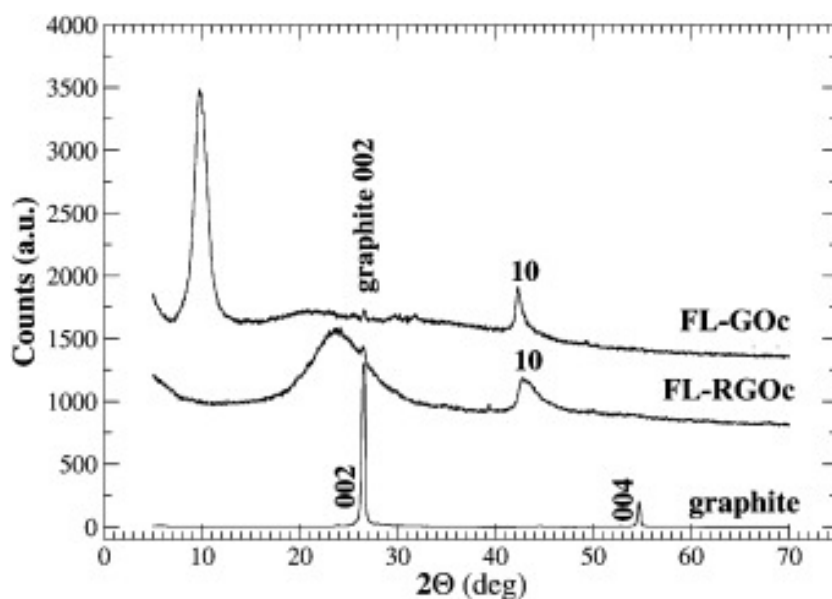


Figure 2.10. XRD spectrum of graphite, graphene oxide and graphene nano sheets [91].

## 2.5. BET (Brunauer-Emmett-Teller) Analysis

Surface area is a very important feature for graphene and its use in applications.  $N_2$  adsorption is widely used to determine the specific surface area of materials. BET (Brunauer-Emmett-Teller) analysis method is used to analyze and evaluate surface area of the materials. BET, however, is not very useful to determine the surface area of graphene because it overestimates the surface area of materials which contain small pores lower than 2 nm down to 1 nm due capillary condensation at relatively low pressures. In addition, the pore volume is also underestimated when pore size is smaller than 0.5 nm [1]. Furthermore, 77.4 K is used as adsorption measurements for nitrogen and it is difficult to measure because filling of 0.5 – 1 nm sizes pores can occur at  $P/P_0$  of  $10^{-7}$  to  $10^{-5}$  where the diffusion rate and adsorption is very slow [85].

## 2.6. FTIR

Surface functional groups have important effect on the properties of synthesized graphene powders. Especially, they generally reduce the electrical conductivity.

FTIR spectroscopy can be used to identify the presence of these surface groups. Generally, the signal around  $1090\text{ cm}^{-1}$  corresponds C-O single bonds,  $1400\text{ cm}^{-1}$  C-OH bonds,  $1600\text{ cm}^{-1}$  due to C=C (aromatic ring),  $1720\text{ cm}^{-1}$  C=O bonds,  $2500$  signal is due to carboxylic acid and at  $1650$  is internal alkene respectively. Figure 4.45 shows the FTIR spectra of graphene oxide and graphene. Graphene oxide has a broad peak at  $3410\text{ cm}^{-1}$  which belongs to OH stretching vibration [90].

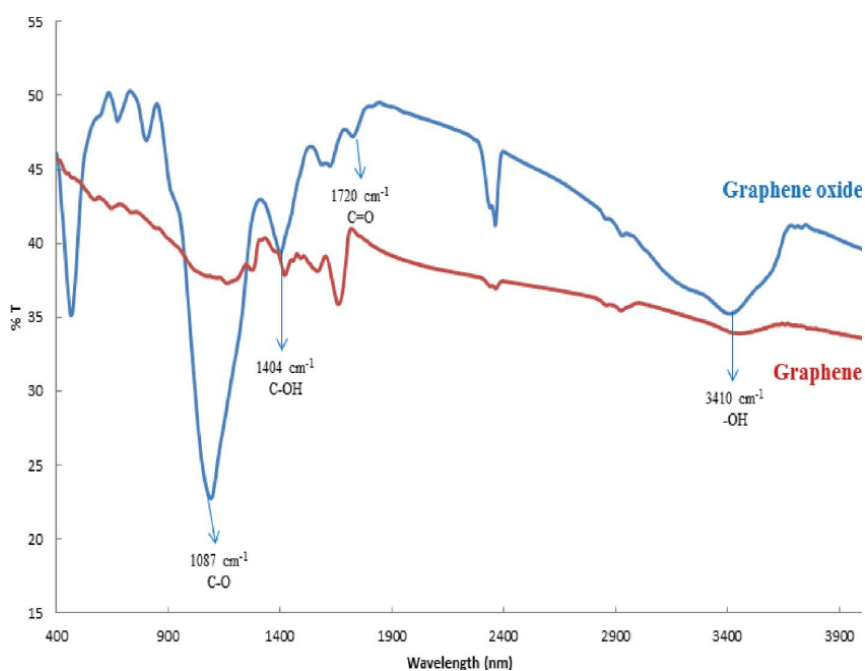


Figure 2.11. FTIR spectrum of graphene oxide and graphene [90].



## CHAPTER 3

### MATERIALS AND METHODS

#### 3.1. Materials

##### 3.1.1. Graphite Rods

Graphite rods that were obtained from Töreci Makine Ticaret were used as both working electrode and counter electrode. The diameter and length of the rod were 10 mm 100 mm, respectively. In addition, its purity was 99% and hardness was 63 shore.

X-Ray diffraction pattern of the as-received graphite used, was given in figure 3.1. There is a sharp diffraction peak at  $26.5^\circ$  which corresponds to the (002) plane and calculated d-spacing is 0.335 nm.

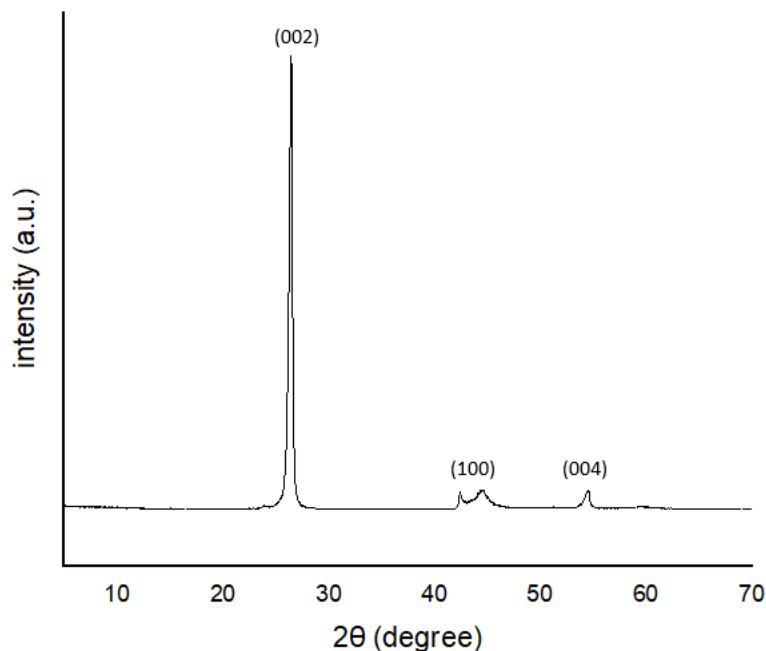


Figure 3.1. XRD spectrum of graphite rod.

### 3.1.2. Chemicals

The electrolyte solutions were prepared with chemicals that are shown in table 3.1. All chemicals were obtained from Sigma Aldrich.

Table 3.1. *Chemicals used in this study.*

Exfoliation agent	Antioxidant agent	Surfactant	Catalyzer agent
H <sub>2</sub> SO <sub>4</sub>	NaOH	CTAB	H <sub>2</sub> O <sub>2</sub>
HNO <sub>3</sub>	KOH	SDS	
NaOH	LiOH		
	NH <sub>4</sub> OH		

#### 3.1.2.1. Exfoliation Agents

Concentration of the exfoliation agent is one of the most important variables which was investigated in this study. Aqueous solutions of H<sub>2</sub>SO<sub>4</sub>, HNO<sub>3</sub>, NaOH were prepared with different molarities. Combination of these chemicals in the electrolyte was also studied. In acidic medium, H<sub>2</sub>SO<sub>4</sub>, HNO<sub>3</sub> were used single or together. The molarity of H<sub>2</sub>SO<sub>4</sub> was varied between 0.12M – 1M; and the molarity of HNO<sub>3</sub> was varied between 0.2M and 0.6M. In basic medium, NaOH, KOH and LiOH was utilized with higher concentrations.

Three different exfoliation agents were utilized in the experiments. These are SO<sub>4</sub><sup>-2</sup>, NO<sub>3</sub><sup>-</sup> and OH<sup>-</sup> ions mainly. H<sub>2</sub>SO<sub>4</sub>, HNO<sub>3</sub> and NaOH were used as source of these ions in the experiments. Among them, SO<sub>4</sub><sup>-2</sup> ion has closest ionic radii to interlayer spacing of graphite. Ionic radii of SO<sub>4</sub><sup>-2</sup>, NO<sub>3</sub><sup>-</sup> and OH<sup>-</sup> ions are 0.258 nm, 0.179 nm and 133 nm respectively [84]. The graphene sheets interplanar spacing is 0.335 nm.

$\text{SO}_4^{2-}$  ions are small enough to fit between graphene layers and big enough to provide efficient exfoliation.

### **3.1.2.2. Antioxidant Agents**

$\text{OH}^-$  ions were utilized in experiments to prevent oxidation of powders. NaOH, KOH, LiOH and  $\text{NH}_4\text{OH}$  were used as source of  $\text{OH}^-$  ions. The molarity of the NaOH was varied between 0.375M-1.5M; KOH was varied between 0.2M-0.375M; LiOH was 1.25M and  $\text{NH}_4\text{OH}$  was 0.2M.

### **3.1.2.3. Surfactants**

Agglomeration is one of the most significant problem of the exfoliation process of the graphene. The graphene powders aggregate due to attractive Van der Waals forces. The powders were not stable in the solution and they were agglomerated both in the solution and after taken from the solution. Surfactants has important effect on surface tension and they were used to prevent agglomeration [88].

Firstly, SDS (Sodium Dodecyl Sulfate,  $\text{NaC}_{12}\text{H}_{25}\text{SO}_4$ ) which is an anionic surfactant was used. SDS has  $\text{SO}_4^-$  as a functional group. It was tried at different concentrations from 100 ppm to 400 ppm but SDS was not enough to prevent agglomeration. The optimum SDS concentration was found as 200 ppm [89].

CTAB (Cetyl Trimethyl Ammonium Bromide,  $\text{C}_{19}\text{H}_{42}\text{NBr}$ ) which is a cationic surfactant was also utilized. CTAB was also tried from 100 ppm to 400 ppm. Higher concentrations than 400 ppm was not used because too much surfactant would decrease the electrical conductivity of graphene [89]. The optimum concentration of CTAB was determined as 400 ppm for aqueous solutions. Also, it is seen that CTAB is more effective to prevent agglomeration of graphene powders.

### **3.1.2.4. Catalyzer**

$\text{H}_2\text{O}_2$  was used in order to increase graphene yield. Its molarity was varied as 0.6M, 0.75M and 1.5M.  $\text{H}_2\text{O}_2$  increases the effectiveness of intercalation with graphite by

producing  $O_2^{2-}$ . It is also utilized as exfoliation agent with high concentrations in some experiments.

### 3.2. Experimental Setup

Two graphite rods were assembled into a cell, such that they are face to face with an adjustable distance between the two. Positive electrode was utilized as the carbon source for the exfoliation process. The experimental cell setup can be seen in figure 3.2.

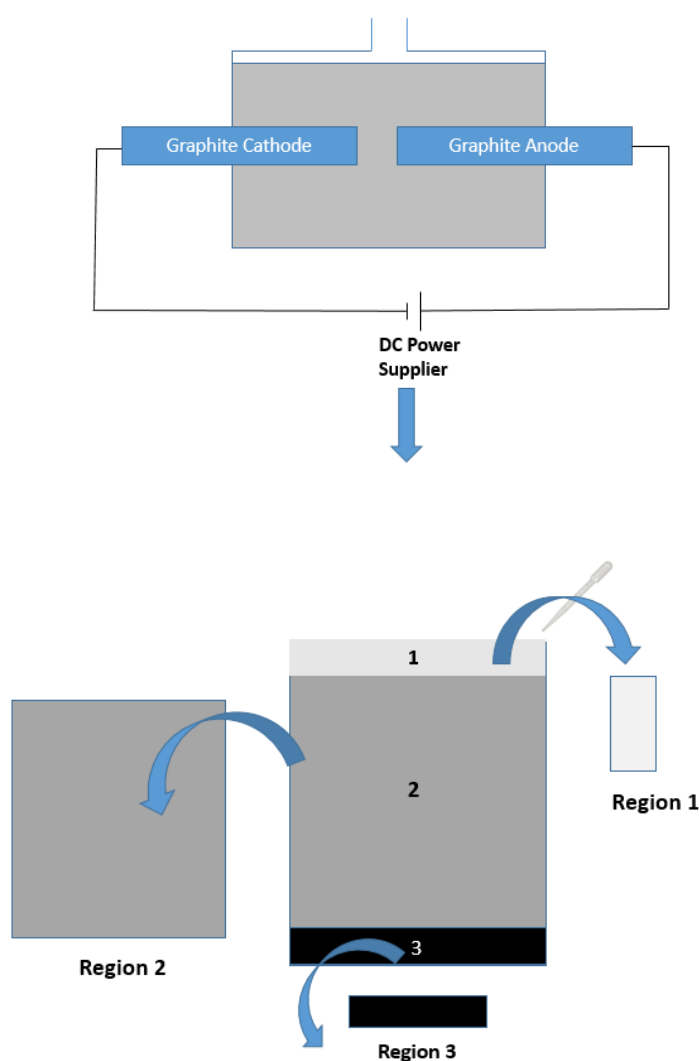


Figure 3.2. Experimental Setup

Electrical power was applied to drive exfoliation process. Experiments were performed with constant current, constant voltage and by changing both voltage and current. Electrical potential (voltage) was changing in the range of -7V and +7V. The exfoliation process occurs mainly in positive electrode because process was performed by negative ions in general.

After finishing the exfoliation process, electrolyte containing the exfoliated graphite particles were transferred to a beaker (see figure 3.3). Due to the nature of the product, there were three regions through the column, which corresponds to floating (region 1), suspended (region 2) and settled (region 3) particles. The highest quality was expected powders which are floating part but their amount was low. The main product was in the suspension region. The quality of the powders were not as high as floating powders. They were taken from the solution by decantation. The settled powders were discarded because their quality was low.

Powders were obtained from region 1 by centrifuge. Powders were centrifuged several times with 9000 rpm for 5 minutes. That process was done many times in order to get rid of the impurities of powders.

Decanted solution (region 2) was then ultrasonicated to disperse graphene. The powders were filtered and washed with distilled several times. Finally, they were deagglomerated in a mixer mill for one minute.

After washing, the filtrate containing the powders passed through the filter was centrifuged at 9000 rpm for 5 min several times. These powders were also considered in region 1 powders. Although the amount is low, highest quality graphene was obtained with this procedure.

As a final operation, all the powders obtained above were dried in vacuum furnace at 200 °C for 5 hours.

### **3.3. Materials Characterization Methods**

#### **3.3.1. SEM**

In this study SEM was used to investigate the morphology of the graphitic structures that were formed after electrochemical exfoliation. FESEM, Nova NanoSEM 430 model was used in ODTU Metallurgical and Materials Engineering Laboratory. Accelerating voltage of 8 kV- 10 kV and 18 kV and spot size 3.5 were used for SEM analysis. Chemical composition analysis was obtained with EDS (Energy Dispersive Spectroscopy).

#### **3.3.2. TEM**

TEM (Transmission Electron Microscopy) was used to determine the crystalline quality of synthesized graphene powders. One drop of sonicated graphene solution was applied on TEM grid and analyzed after drying.

#### **3.3.3. X-Ray**

In this study, X-Ray analysis was used to investigate structural changes in graphitic structure. XRD analysis was carried out by XRD, Bruker D8 Advance device. Diffraction data was collected within the 2-theta ( $\theta$ ) range of 5-90°, with a scan rate of 1°·min<sup>-1</sup>.

#### **3.3.4. BET (Brunauer-Emmett-Teller)**

. BET (Brunauer-Emmett-Teller) analysis method is used to analyze and evaluate surface area of the materials. AUTOSORB-1C/MS was used in ODTU-MerLab for measurements. N<sup>2</sup> adsorption was applied at 77.40K in the pressure range of 0.08 to 0.3 for this analysis.

#### **3.3.5. Raman Spectroscopy**

Raman spectrum was used in order to indicate characteristic of disordered carbon structure. Renishaw inVia was used in ODTU-MerLab for measurements. 532 nm laser was used in the analysis.

### **3.3.6. FTIR Analysis**

Surface functional groups were analyzed with FTIR analysis in this study. FTIR analysis was carried out by Varian- Cary 100 Bio UV-Visible Spectrophotometer.



## CHAPTER 4

### RESULTS, CHARACTERIZATION AND DISCUSSIONS

#### 4.1. Parameters of Experiments

In this work, effects of processing parameters for electrochemical exfoliation method of graphene production were studied. These parameters are:

- Current
- Exfoliation agents: concentrations and types
- Catalyzer
- Antioxidant agents
- Surfactants

Type and concentration of exfoliation agent, current and voltage amounts, surfactant type and amount and antioxidant agents are the most important parameters of the experiments. Experiment parameters were given in table 3.3.

After the process, formed slurry is investigated in three regions: Region 1 (floating particles), Region 2 (suspended particles), Region 3 (settled particles). The graphitic particles from three different regions were collected as described in experimental procedure part and their amount are determined by weighting in table 4.1.

Addition to these three regions also, there are some particles passed through filter. Amount of these powders are very low. These powders were studied in below chapter.

Table 4.1. *Experiments*

Exp No	Exfoliation Agent			Antioxidant Agent			Catalyzer	Surf.		I (A)	V	ph	Amount (g)			
	H <sub>2</sub> SO <sub>4</sub>	HNO <sub>3</sub>	H <sub>2</sub> O <sub>2</sub>	NaOH	LiOH	KOH		NH <sub>4</sub> OH	H <sub>2</sub> O <sub>2</sub>				SDS	CTAB	Fl.	Susp.
1	-	-	0.6M	1.5M	-	-	-	-	250	-	0.30	5.0	13.40	0.28	0.73	0.96
2	0.25M	-	-	0.375M	-	-	-	0.75M	-	250	0.50	5.5	1.99	0.06	0.69	0.6
3	0.25M	-	-	0.375M	-	-	-	0.75M	-	400	0.35	5.5	1.99	0.08	0.1	0.23
4	0.25M	-	-	-	1.25M	-	-	0.75M	-	400	0.20	5.5	11.10	0.2	0.12	0.13
5	0.25M	-	-	-	-	-	-	1.5M	200	-	0.20	2.5	1.20	0.16	0.88	1.65
6	0.3M	-	-	-	-	0.375M	0.2M	0.75M	200	-	0.30	3.0	8.11	0.3	0.51	4.02
7	0.5M	-	-	0.375M	-	-	-	0.75M	-	250	0.20	5.0	1.72	0.27	1.25	1.46
8	-	0.4M	-	0.375M	-	-	-	0.75M	-	250	0.20	5.0	12.30	0.08	0.1	0.23
9	1M	0.6M	-	-	-	-	-	-	-	500	0.30	2.5	0.95	0.29	1.02	1.66
10	0.2M	0.3M	-	-	-	0.2M	0.2M	-	-	200	0.50	3.0	1.19	0.46	1.57	2.31
11	0.25M	0.4M	-	0.375M	-	-	-	0.75M	-	400	0.55	7.5	1.70	0.18	0.57	2.44
12	0.25M	0.4M	-	0.375M	-	-	-	0.75M	-	400	0.27	6.0	1.70	0.17	0.86	1.31
13	0.12M	0.2M	-	0.375M	-	-	-	0.75M	-	400	0.10	5.5	3.42	0.32	0.45	0.28
14	0.25M	0.4M	-	0.375M	-	-	-	0.75M	-	400	0.15	5.0	1.70	0.23	1.64	1.39
15	0.25M	0.4M	-	0.45M	-	-	-	0.75M	-	400	0.20	4.5	3.42	0.17	0.14	0.2
16	0.25M	0.4M	-	-	-	-	0.2M	0.75M	-	400	0.20	5.0	2.29	0.43	0.98	0.9

Fl\*: floating, Susp\*:suspended, Sett\*: settled

Figure 4.1 shows the SEM images of the particles that were obtained from region 1, 2 and 3. It can be seen that the region 1 and 2 give more promising results for graphene forming. It is observed that the particles in region 3 are bigger and thicker than region 1 and 2.

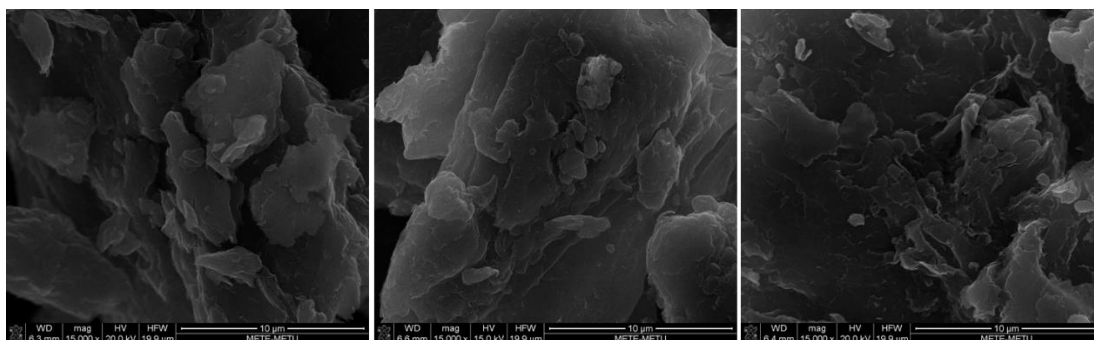


Figure 4.1. SEM images of region 1, 2 and 3 from experiment 10.

## 4.2. Studies on the Filtered Particles

The particles passed through the filter are investigated in SEM (Fig. 4.2 and Fig. 4.3). It is seen that these particles are generally equiaxed or spherical particles, with diameters ranging from 30 nm to 150 nm.

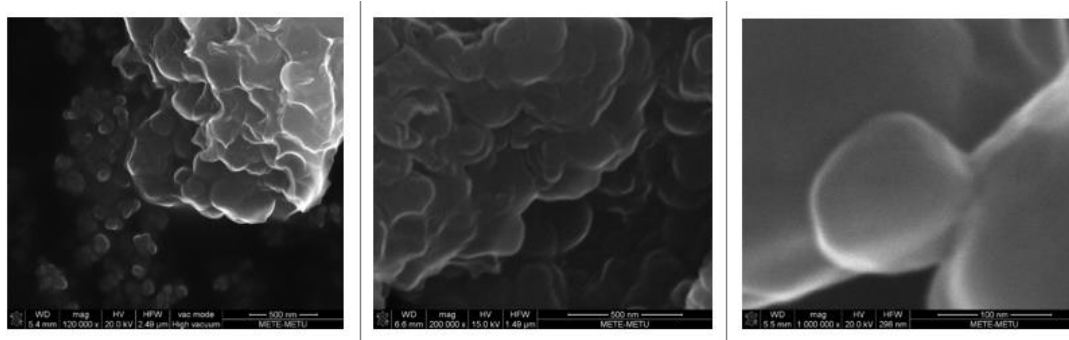


Figure 4.2. SEM images of filtered particles

The powders which is seen in figure 4.3 were obtained from experiment 10. The solution was centrifuged 5 times with 9000 rpm and 10 minutes. The average

particle size of these powders were measured as 120 nm. They are observed to be homogeneously shaped and fine.

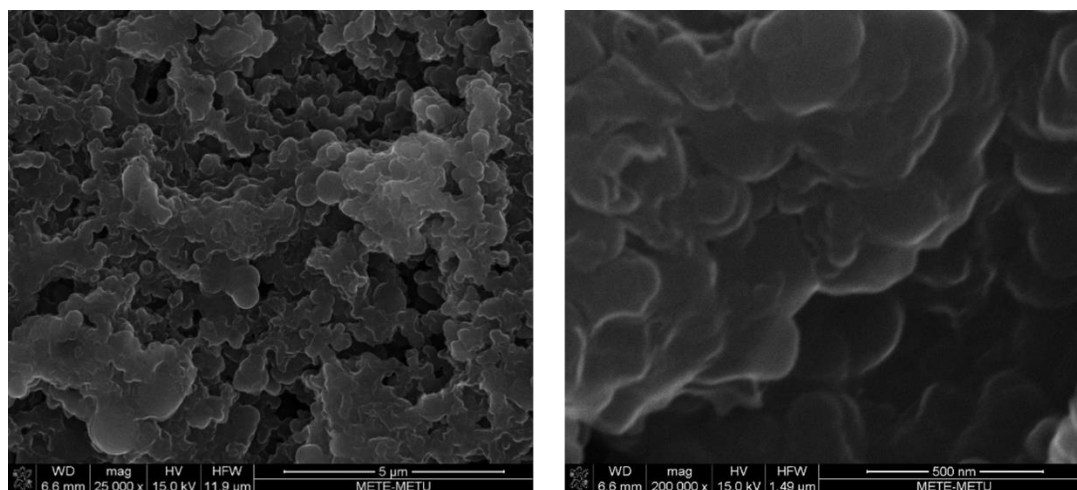


Figure 4.3. SEM images of experiment 10

Surface properties and mean thickness of synthesized graphene powders were investigated by Atomic Force Microscopy. AFM analysis were done to discover the number of layers of the graphene by investigating sheet thickness of it.

As seen in figure 4.4, the thickness of the graphene sheets was investigated in  $1 \mu\text{m}^2$  area. In figure 4.4, thickness measurements were done along 3 different paths. The important point is that, the powders were agglomerated and the measured thickness does not belong to a single graphene particle. In green path, there were 3 different graphene powder groups and their height are 15 nm, 40 nm and 35 nm.

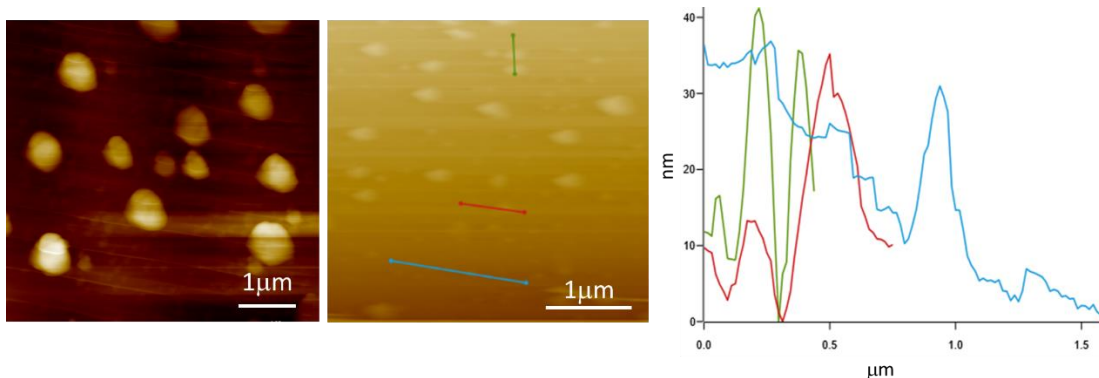


Figure 4.4. Thickness measurements of particles with AFM.

Thin flake like structures are mostly found in region 1, therefore, throughout this study we focused on the structures collected from region 1.

### 4.3. Effects of Exfoliation Agent and Antioxidants

Experiments were performed using:

- only NaOH,
- only H<sub>2</sub>SO<sub>4</sub>,
- only HNO<sub>3</sub>, and
- H<sub>2</sub>SO<sub>4</sub> and HNO<sub>3</sub> together as exfoliation agent.

Further current effect was studied in some experiments which have promising results.

EDS analysis showed that powders have different chemical impurities according to type of used exfoliation agent and antioxidant agent. Therefore, according to the field of application, selected exfoliation agent is also important in this respect.

Elemental analysis of the powders was done by EDS. Table 4.2. shows the chemical compositions of the synthesized graphene powders. These results are taken from average EDS results of each experiments which is analyzed at more than 50000

magnifications. Even though washing and filtering were done, there still remains S, Na and K impurities in powders from antioxidant agents and H<sub>2</sub>SO<sub>4</sub>.

Table 4.2. EDS results of the experiments.

Exp	S (wt. %)	Na (wt. %)	K (wt. %)
1		5.66	
2		1.52	
3	1.45	2.02	
4	5.02		
5	5.94		
6	2.07		3.88
7	1.33	0.81	
8		4.08	
9	6.88		
10	0.38		1.50
11	0.74	3.27	
12	1.05	4.13	
13	1.13	4.43	
14	1.27	0.54	
15	2.39		
16	0.82		

#### 4.3.1. Experiments with NaOH

Generally in acidic environment, the intercalation of the agents is strong so a lot of graphite particles may drop without completing their exfoliation process laterally. The intercalation is not that much strong in basic solutions, so particles may have more opportunity to complete their exfoliation process. In order to test this and observe exfoliation process in basic electrolyte, NaOH was used as exfoliation agent (Experiment number 1 in Table 4.1). Figure 4.3 shows the SEM image and XRD spectrum of particles which were synthesized by using 1.5 M NaOH and H<sub>2</sub>O<sub>2</sub> solution.

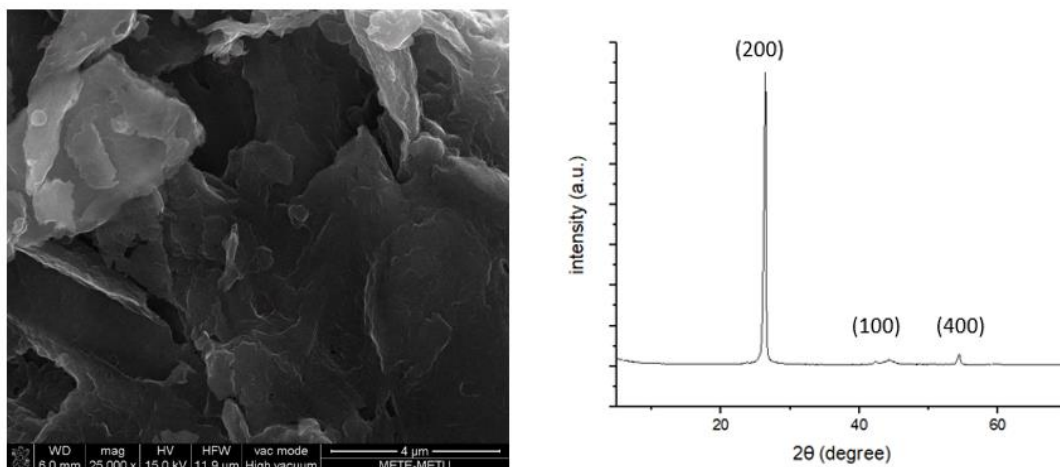


Figure 4.5. (a) The SEM image of particles), (b) XRD Spectrum of particles with 1.5M NaOH (exp 1

The particles obtained from region 1 is given in Fig 4.5 planar structure (Fig a). Furthermore XRD result showed that the particles were graphitic. The XRD spectrum of experiment 1 is given in figure 4.5(b). It can be seen that the spectrum is not much different from spectrum of graphite. Therefore, the product of this experiment was more close to graphitic structure than graphene structure.

### 4.3.2. Experiments with H<sub>2</sub>SO<sub>4</sub>

#### 4.3.2.1. With Antioxidant Agent NaOH

In some experiments, only H<sub>2</sub>SO<sub>4</sub> was used as exfoliation agent and concentration, voltage and current effects on the morphology were investigated. SO<sub>4</sub> is used as main exfoliation agent for these experiments.

3 different experiments' SEM images can be shown in figure 4.6, 4.7 and 4.8. In order to see the effect of current, 0.5 A, 0.35 A and 0.2A were applied in 0.25M H<sub>2</sub>SO<sub>4</sub> solution.

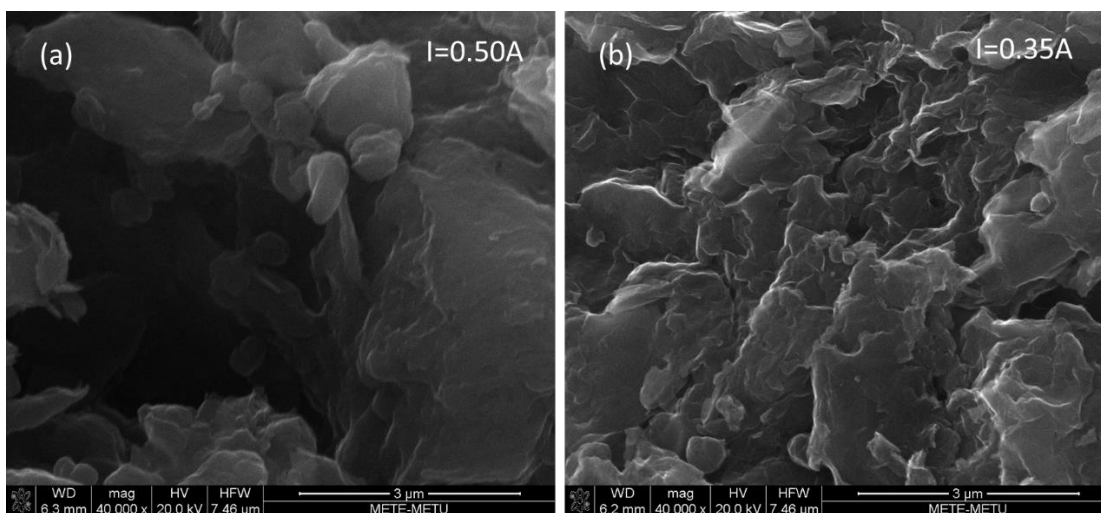


Figure 4.6. The SEM images of particles with (a) 0.25M  $H_2SO_4$  with 5.5V and 0.5A (exp 2), (b) 0.25M  $H_2SO_4$  with 5.5V and 0.35A (exp. 3).

#### 4.3.2.2. With Antioxidant Agent LiOH

It is seen that as current decreases, the morphology changes from equiaxed particles to flake-like structures. Graphene flakes were observed when current was applied as 0.2A. In figure 4.7, SEM images and XRD spectrum of particles were given.

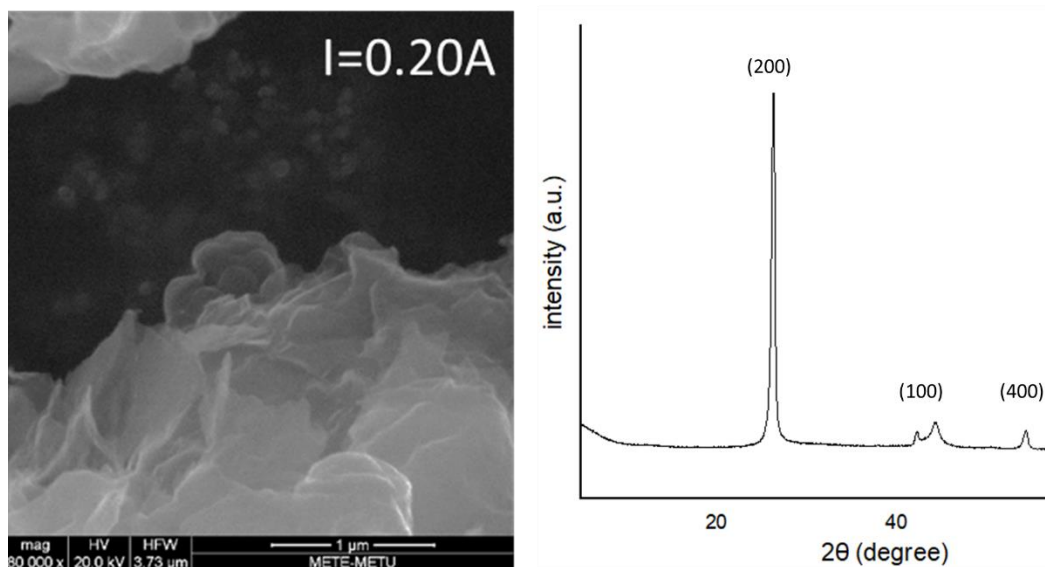


Figure 4.7. (a)The SEM images, (b) XRD spectrum of graphene particles with 0.25M  $H_2SO_4$  with 5.5V and 0.2A (exp. 4).

### 4.3.2.3. With Antioxidant Agent KOH and NH<sub>4</sub>OH

In figure 4.8, SEM images were taken from the middle region of the powders. The powder shapes and size are similar and homogeneous. The images in figure 4.12 were taken from the edge region of graphene sheets. Since they are at edge, they look more transparent in image. Both samples were taken from region 1.

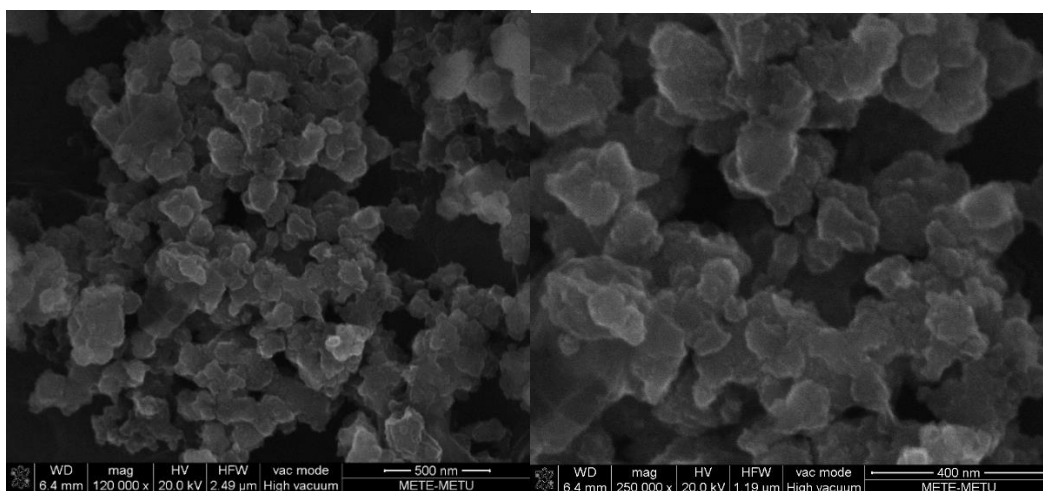


Figure 4.8. The SEM images of particles with 0.3M H<sub>2</sub>SO<sub>4</sub> with 3V and 0.3A (exp 6).

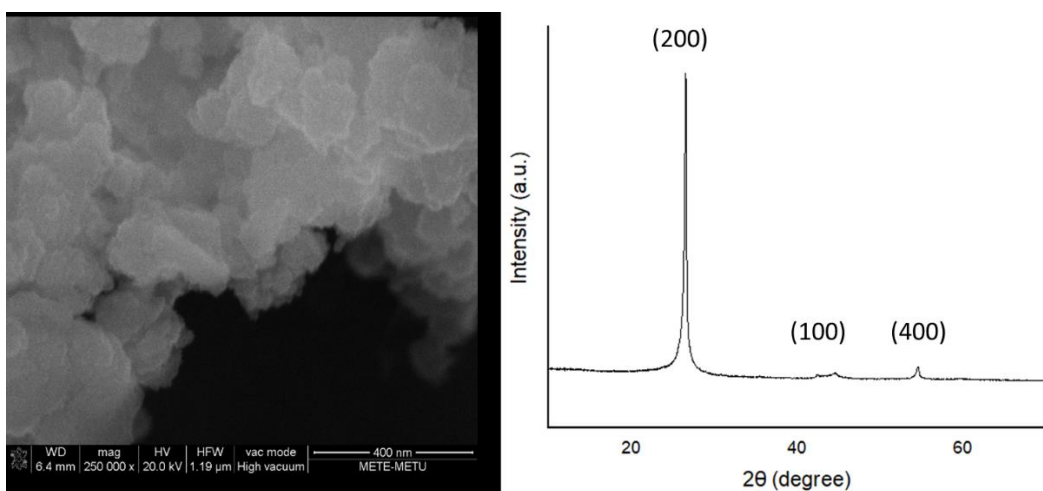


Figure 4.9. The SEM images of graphene particles with in edge region and XRD spectrum of particles , 0.3M H<sub>2</sub>SO<sub>4</sub> with 3V and 0.3A (exp. 6).

In figure 4.9, XRD spectrum of experiment 6 is given. The main peak is broader than graphite peak, so it can be said that powder structure is in between graphite and graphene.

### 4.3.3. Experiments with HNO<sub>3</sub>

HNO<sub>3</sub> is another exfoliation agent which was studied. When HNO<sub>3</sub> was used as exfoliation agent, the particle size was coarser than H<sub>2</sub>SO<sub>4</sub>. This can be seen in figure 4.10. XRD spectrum of the particles are similar to spectrum of graphite.

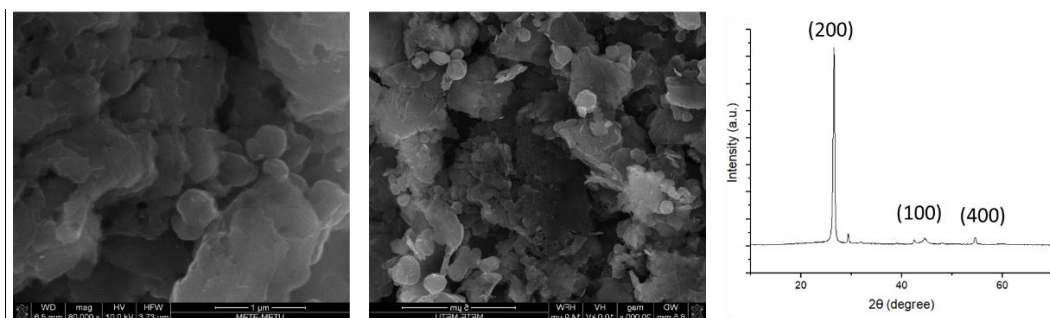


Figure 4.10. The SEM images and XRD spectrum of particles with HNO<sub>3</sub> were used as exfoliation agent (exp 8).

### 4.3.4. Experiments with H<sub>2</sub>SO<sub>4</sub> / HNO<sub>3</sub>

#### 4.3.4.1. The Effect of Current

In this study, the effect of current was investigated by keeping all other variables constant and changing the current to 0.55 A, 0.27 A and 0.15 A in experiment 11, 12 and 14 (Table 4.1). SEM images of the particles which are collected from region 1 are given figure 4.11 comparatively.

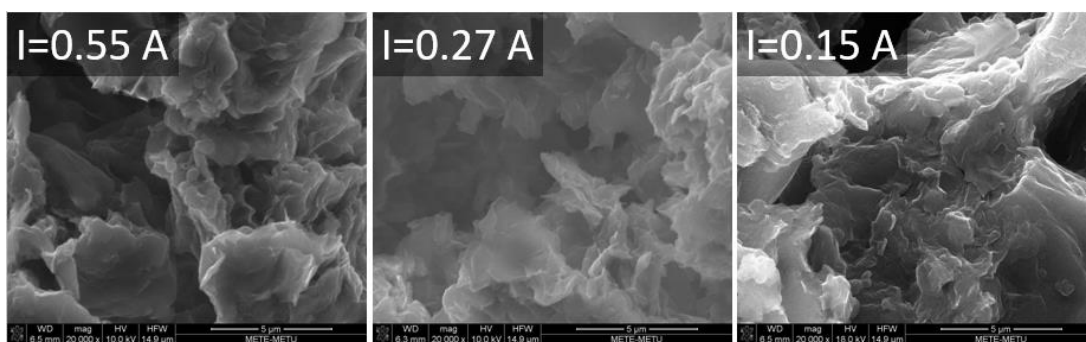


Figure 4.11. SEM images of the powders obtained with current 0.55A, 0.27A and 0.15A.

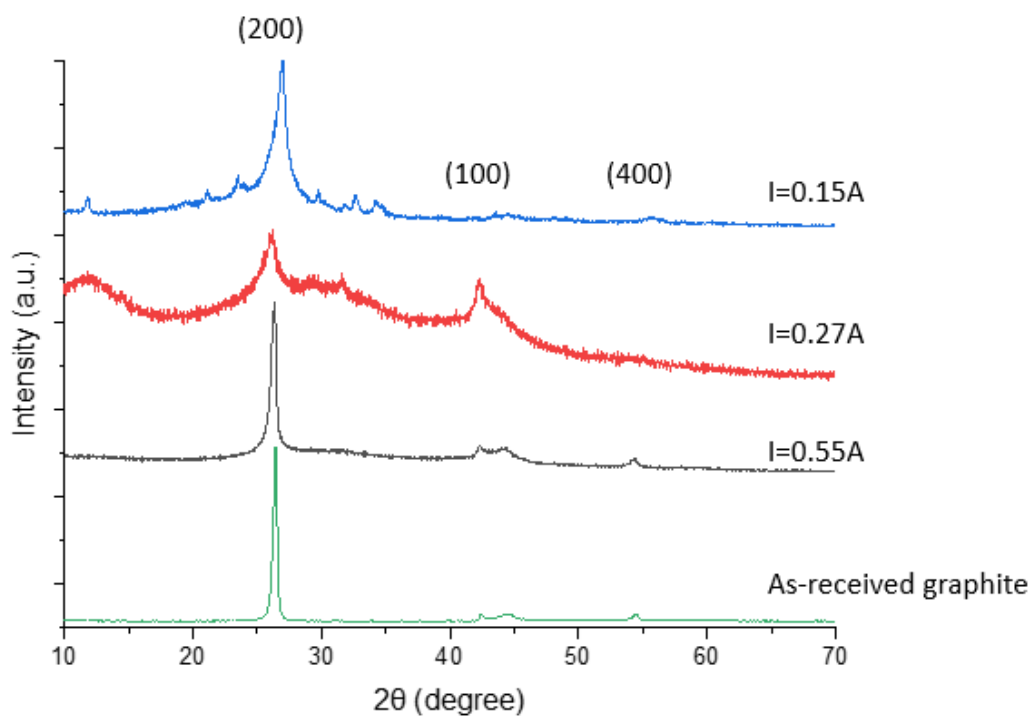


Figure 4.12. XRD spectrum of As-Received Graphite Rod, Experiments 11,12 and 14.

In figure 4.12, XRD spectrum of experiments and graphite rod were given. It can be said that the XRD result of graphite rod and experiment 11 ( $I=0.55A$ ) are similar to each other. The results of experiment 12 ( $I=0.27A$ ) and experiment 14 ( $I=0.15A$ ) are closer to XRD spectrum of graphene. (see figure 2.10)

In order to investigate the effect of current, the amount of powders was measured and the exfoliation rate is calculated according to eqn 8:

$$\text{Exfoliation Rate (ER)} = \frac{\text{Amount of Exfoliation Products (mg)}}{\text{Time (h)}} \dots\dots\dots(8)$$

Table 4.2. *Current Effect on Exfoliation Rate.*

<b>Exp</b>	<b>I (A)</b>	<b>Exfoliation Rate (mg/hr)</b> (Based on formation of Floating-R1 and Suspended-R2 particles)	<b>Exfoliation Rate</b> (Based on total powder)	<b>Ratio of R1+R2 / Total Powder</b>
14	0.15	37.3	65.1	0.57
12	0.27	32.1	72.8	0.44
11	0.55	31.0	132.5	0.23

Higher current causes increasing amount of total powders. On the other hand, since the reaction rate is increasing with current, controlling of the reaction mechanism becomes more difficult due to fast kinetics of the reaction. Generally, homogeneity and quality of the powders are higher at lower currents. Current effect on exfoliation rate of both quality graphene (floating graphene and suspended graphene) and total graphene can be seen in table 4.2 and figure 4.13. Quality of the experiments is dependent the ratio of floating and suspended graphene to total powders. That is given in equation 9.

It can be seen that exfoliation rate of quality graphene is higher at lower current density but total ER is higher at higher current density. In experiment 14, almost half of the powders have high quality. The ratio of high quality graphene to total powder is decreasing with the increasing of current.

$$\text{Quality} = \frac{\text{Total amounts of floating and suspended powder}}{\text{Total amount of powder}} \dots\dots\dots(9)$$

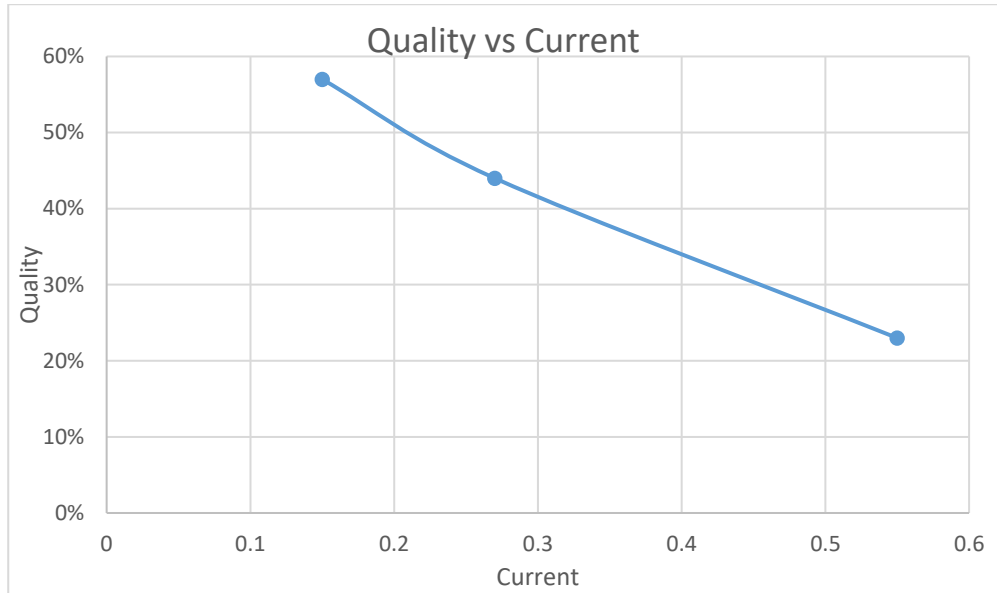


Figure 4.13. Current effect on quality of the powders

In figure 4.14, the percentage of floating, suspended and settled powders were given. It is clearly seen that percentage of floating + suspended powders are increasing with decreasing of the current.

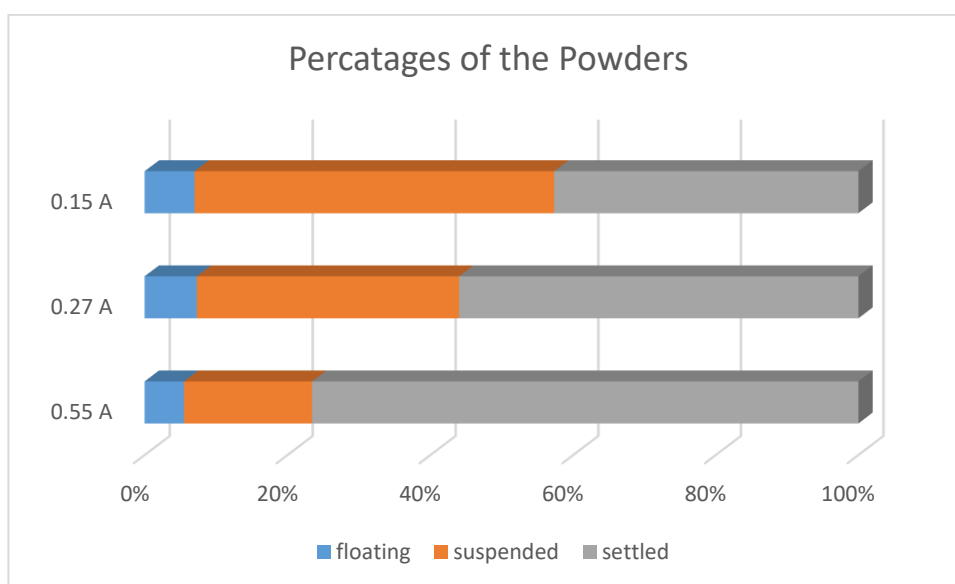


Figure 4.14. Percentages of floating, suspended and settled powders.

#### 4.3.4.2. The Effect of the molarity of Exfoliation Agent

In order to understand the effect of the molarity of exfoliation agent, other parameters were kept constant and amounts of the exfoliation agents were changed in experiment 13 and 14. The results were given in table 4.3

Table 4.3. Effect of exfoliation agent on E.R.

Exp	Exf agent	Exf. Agent	E.R. (Region 1 and 2) (mg/h)	E.R. (total powder) (mg/h)
13	0.125M H <sub>2</sub> SO <sub>4</sub>	0.2M HNO <sub>3</sub>	11.24	15.39
14	0.25M H <sub>2</sub> SO <sub>4</sub>	0.4M HNO <sub>3</sub>	37.23	65.10

The exfoliation rate of graphene is increasing more than 3 times when the exfoliation agent was doubled. The SEM images of experiment 13 and 14 were given in figure 4.15.

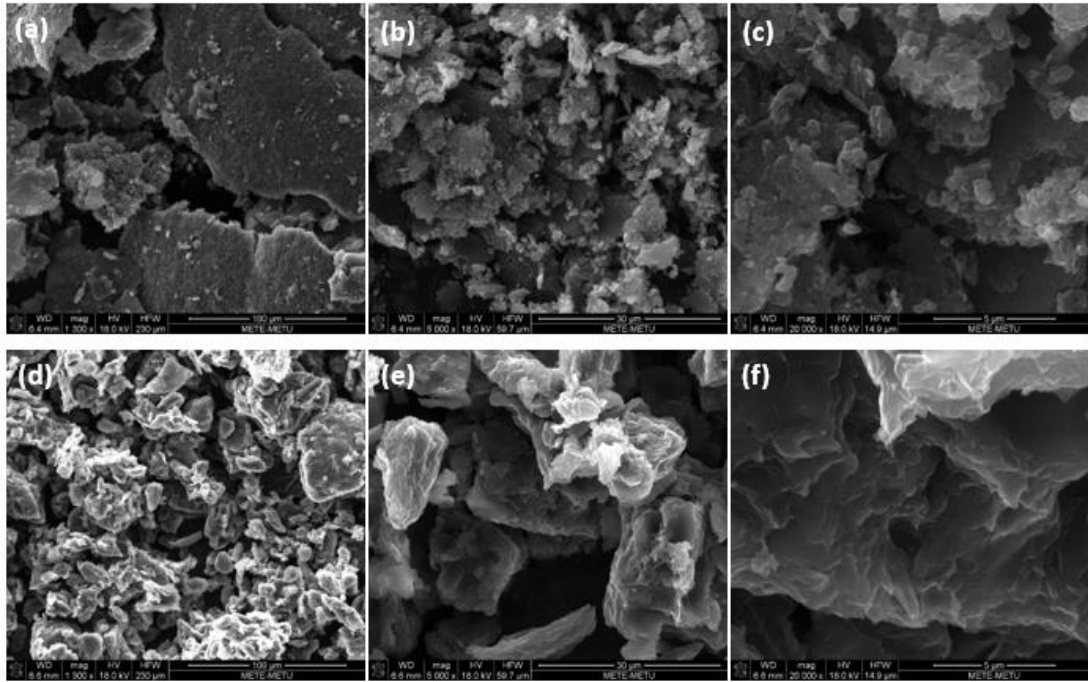


Figure 4.15. SEM images of Region 2 a-c) Experiment 13, d-f) Experiment 14

The results of experiment 14 were more promising than the other experiments. Since, experiment 14 was analyzed in more detail. In figure 4.6, SEM and Raman spectroscopy results of the structures taken from the region 1 of the experiment 14 were given.

In figure 4.16, SEM image and Raman Spectrum of experiment 14 were given.

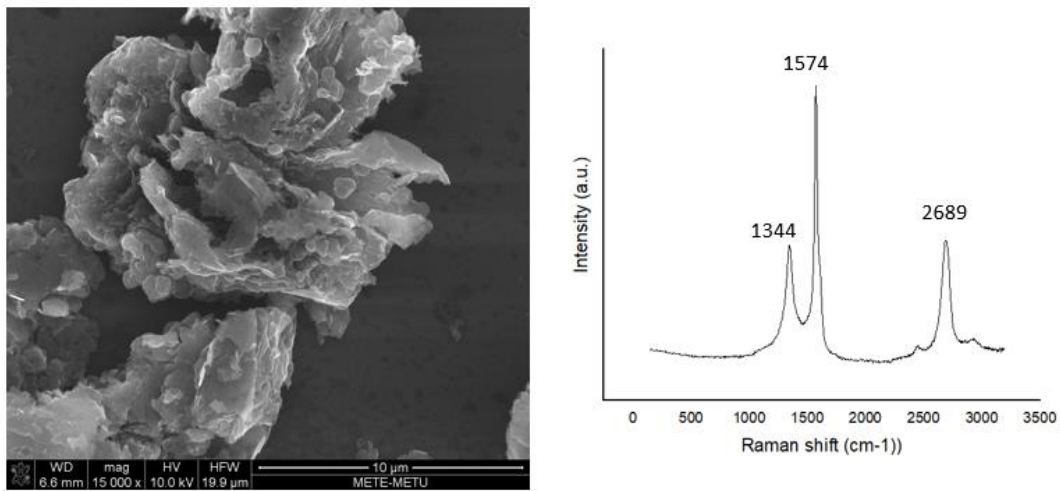


Figure 4.16. SEM and Raman Spectroscopy results of region 1 of the experiment 14.

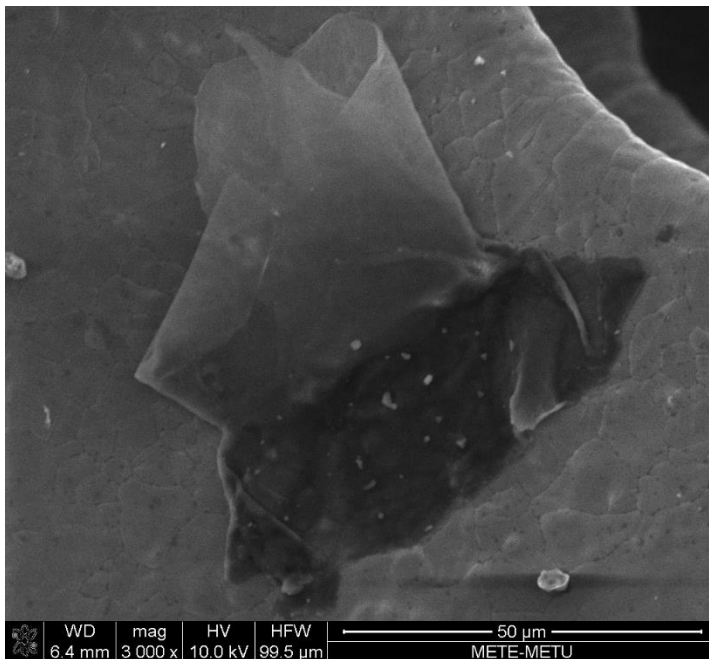


Figure 4.17. The SEM images of graphene particles with 0.25M  $H_2SO_4$ , 0.4M  $HNO_3$ , 5.5V and 0.15A (exp. 14).

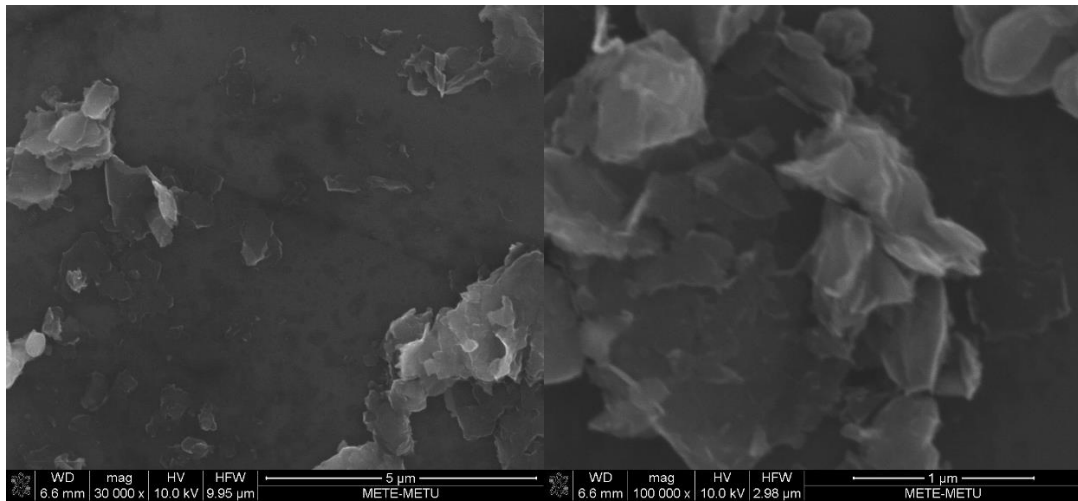


Figure 4.18. The SEM images of graphene particles with 0.25M  $H_2SO_4$ , 0.4M  $HNO_3$ , 5.5V and 0.15A (exp. 14).

In figure 4.17 graphene flakes is seen as wrinkled folded. The morphology of powders is observed in figure 4.18. There are a lot of graphene flakes, but they are generally agglomerated.

Figure 4.19 shows XRD spectrum of the experiment 14 and experiment 13. In experiment 14, there is a peak around  $12^\circ$  which belong to graphene oxide. Another peak is observed at  $26^\circ$  which is a broad graphene peak for both experiments. In addition, there is another peak slightly shifts to left when compared to graphite peak. That peak may show the property of graphene.

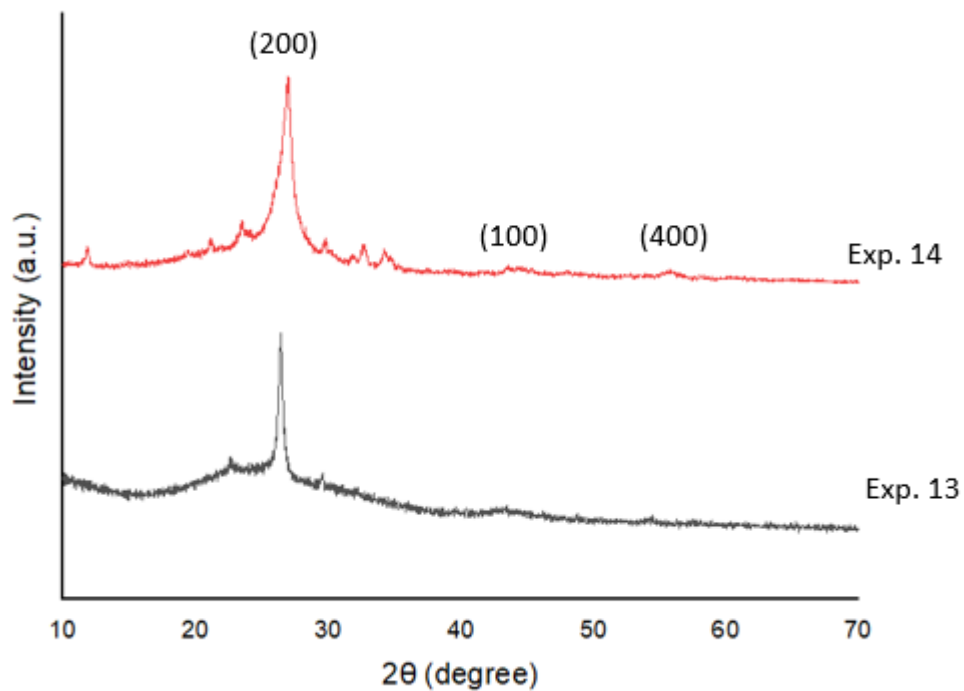


Figure 4.19. XRD Spectrum of Experiment 14 and Experiment 13.

BET analysis was used to determine the specific surface area of synthesized graphene powders. Relatively lower pressures were chosen in this study because it is reported that lower pressures give more accurate results for BET analysis [86]. Pressure range is determined as 0.08 to 0.3 for BET analysis for BET surface area analysis in this study.

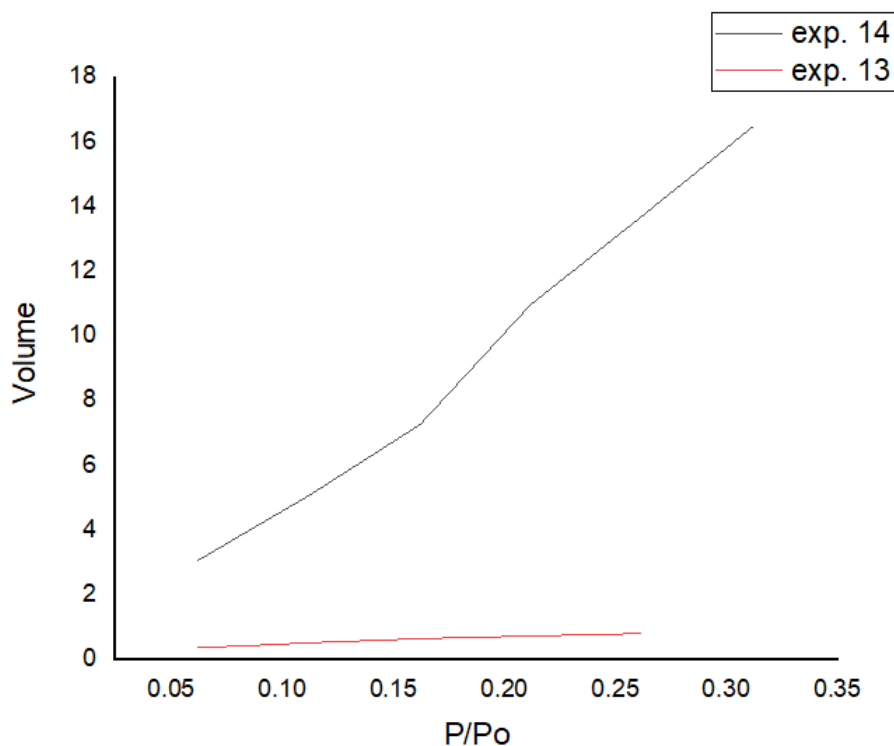
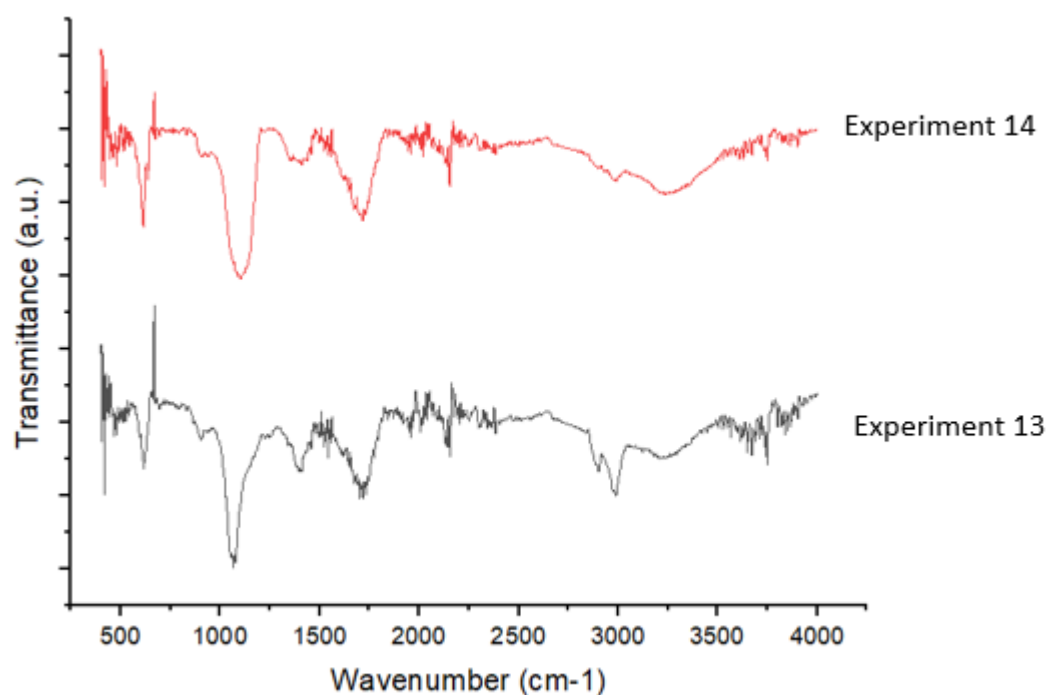


Figure 4.20. BET analysis of experiment 13 and 14.

Figure 4.20 shows the adsorption isotherms of the experiment 13 and 14. Specific surface areas of the experiments were calculated as 3.16 m<sup>2</sup>/g and 110.6 m<sup>2</sup>/g respectively. According to these results, it can be said that the specific surface area of the powders is low when the molarities of the exfoliation agents are low (experiment 13). On the other hand, specific surface area of synthesized graphene was measured as 110 m<sup>2</sup>/g in experiment 14 which is the best results in all experiments.

Figure 4.21 shows the FTIR spectrum of the experiment 13 and experiment 14. Both of powders show peaks which are C-O stretching around 1100 cm<sup>-1</sup>, CO-H bending around 1400 cm<sup>-1</sup>, C=C stretching around 1600 cm<sup>-1</sup> and CO-H stretching around

3350  $\text{cm}^{-1}$ . The intensities of the peaks are small and this indicates that the amount of the inserted oxygen groups is low.



*Figure 4.21. FTIR spectrum of the experiment 13, experiment 14.*

#### **4.3.4.3. With No Antioxidant Agent**

The  $\text{H}_2\text{SO}_4$  and  $\text{HNO}_3$  were utilized together as exfoliation agent chemical in experiments. Firstly, they are tried at high molarities as  $\text{H}_2\text{SO}_4$  was 1M and  $\text{HNO}_3$  was 0.6M.

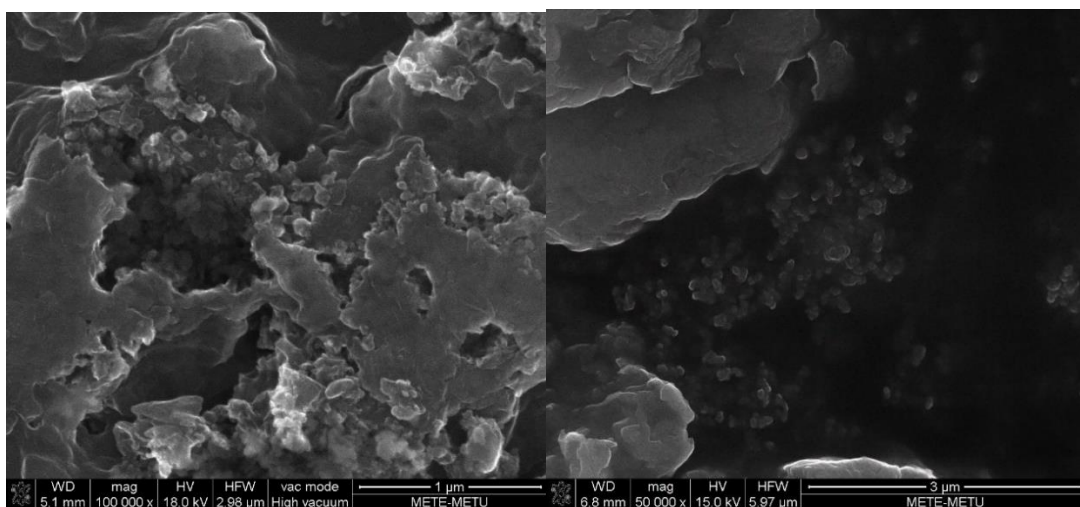


*Figure 4.22. The SEM images of particles with 1M H<sub>2</sub>SO<sub>4</sub> and 0.6M HNO<sub>3</sub> were utilized together with 2.5V and 0.3A (exp. 9).*

SEM images of figure 4.22 shows that there were coarse and fine particles together in the synthesized graphene powders. The finest particle size was achieved in this experiment but oxidation was also really high.

XRD spectrum of experiment 9 was given in figure 4.23. It is observed that there is a graphene oxide peak at 14° in that graph. No chemicals like NaOH or KOH were used in this experiment to prevent oxidation. As a result, the powders were obtained as graphene oxide mostly. In addition, graphene peak was also observed.

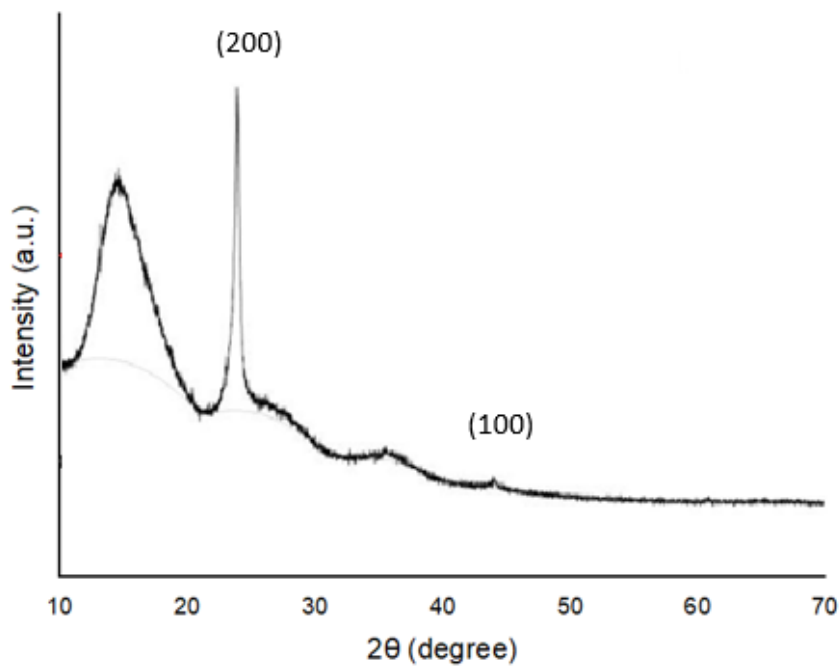


Figure 4.23. XRD Spectrum of GO Peak in Experiment 9.

#### 4.3.4.4. With Antioxidant Agent KOH

At lower current ( $I=0.2A$ ), the structure becomes more flake like. In addition, XRD spectrum of particles are more like XRD spectrum of graphene. SEM image and XRD spectrum of experiment 15 was given in figure 4.24. In this experiment, current was low and so reaction kinetic was low as well. Thus, reactions take places slowly.

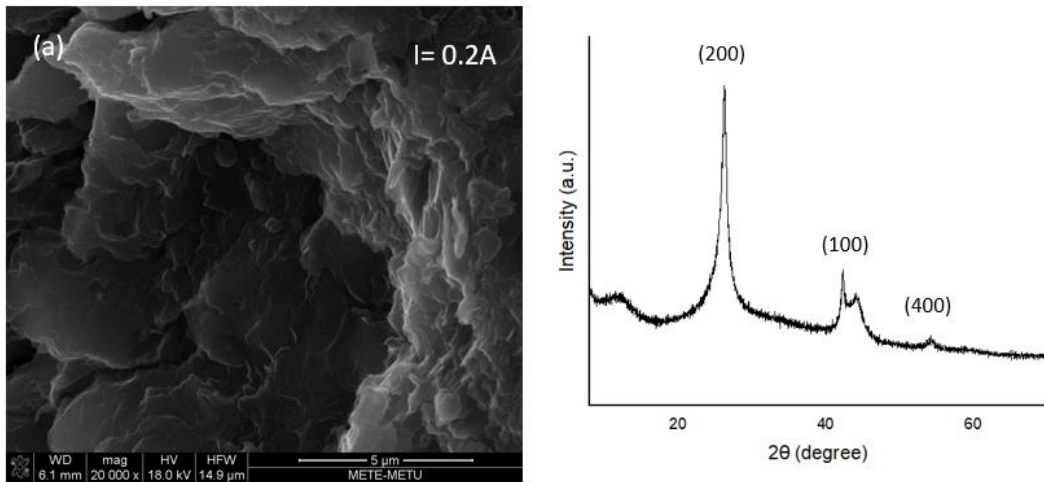


Figure 4.24. The SEM image and XRD spectrum of particles with 0.25M  $H_2SO_4$  and 0.4M  $HNO_3$  with 4V and 0.2A (experiment 15)

When they are used at lower concentration, less oxidation was observed in powders. The graphene powders that is seen in figure 4.25 were obtained with the experiment which is done by 0.2M  $H_2SO_4$  0.3M  $HNO_3$  with 3V and 0.5A. The graphene powders in figure 4.25 are flake shape particles. The flakes have some transparency as well. They are taken from solution by washing with distilled water, filtering and then drying in vacuum furnace. They are observed to be homogeneously shaped and fine.

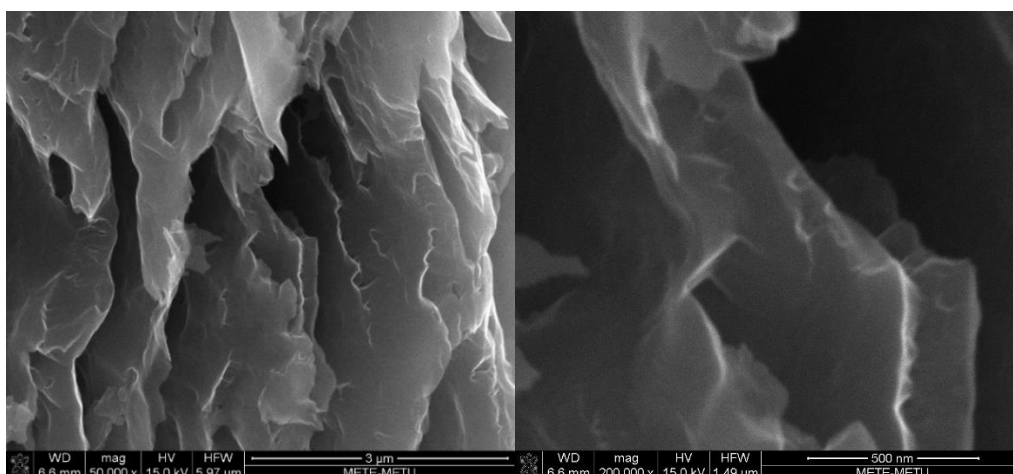
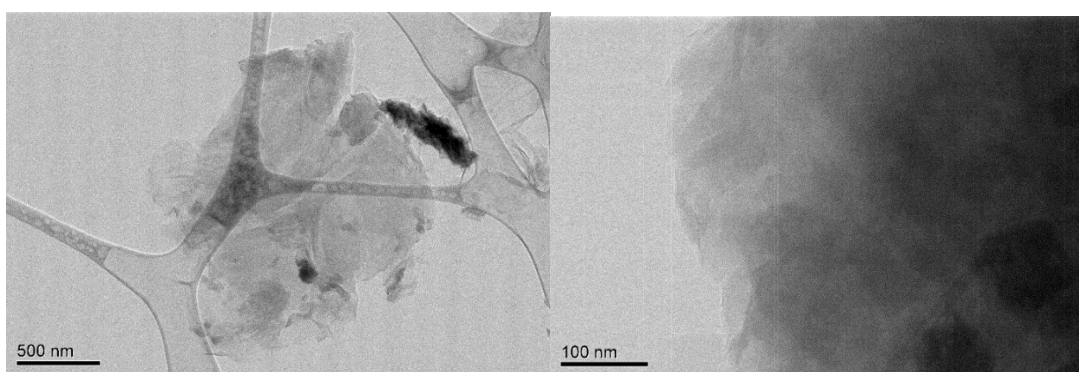


Figure 4.25. The SEM images of graphene particles with 0.2M  $H_2SO_4$  and 0.3M  $HNO_3$  with 3V and 0.5A (exp. 10).

TEM (Transmission Electron Microscopy) is utilized to determine the crystalline quality of synthesized graphene powders. One drop of sonicated graphene solution was applied on TEM grid and analyzed after drying. Some large flakes which is about 1-2  $\mu m$  was seen during analysis. In addition, folded edges was observed in flakes.



(a)

(b)

Figure 4.26. The TEM images of graphene sheets for experiment 10.

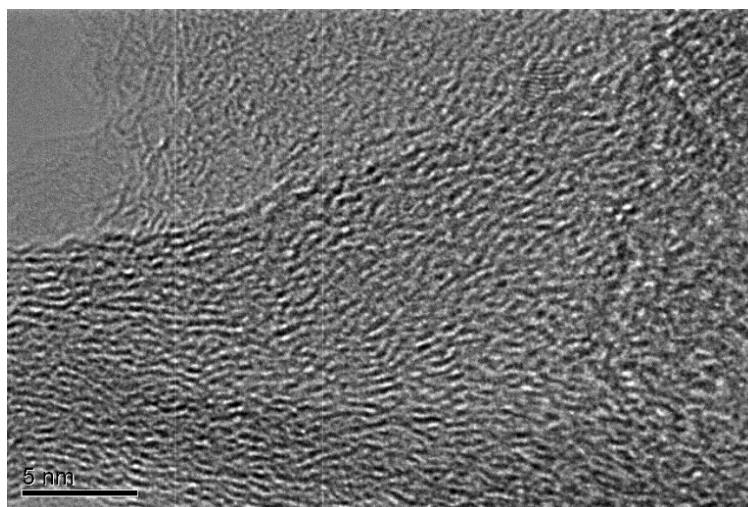


*Figure 4.27. Graphene layers in TEM image for experiment 10.*

Figure 4.27 shows TEM images of the exfoliated graphene sheets. The average lateral size of graphene sheet was 1  $\mu\text{m}$ .

The interlayer distance obtained from TEM image in figure 4.32 obtained about 0.42 nm that is larger than interlayer distance of graphite which is 0.335 nm. So it can be said that almost 30 % expansion was occurred in between graphite layers.

#### **4.3.4.5. With Antioxidant Agent $\text{NH}_4\text{OH}$**

$\text{NH}_4\text{OH}$  was also used in experiments as antioxidant agent. When other parameters were kept constant and  $\text{NH}_4\text{OH}$  was used, powders were obtained finer. Flake like structures were observed in experiment 16. SEM images of experiment 16 were given in figure 4.28.

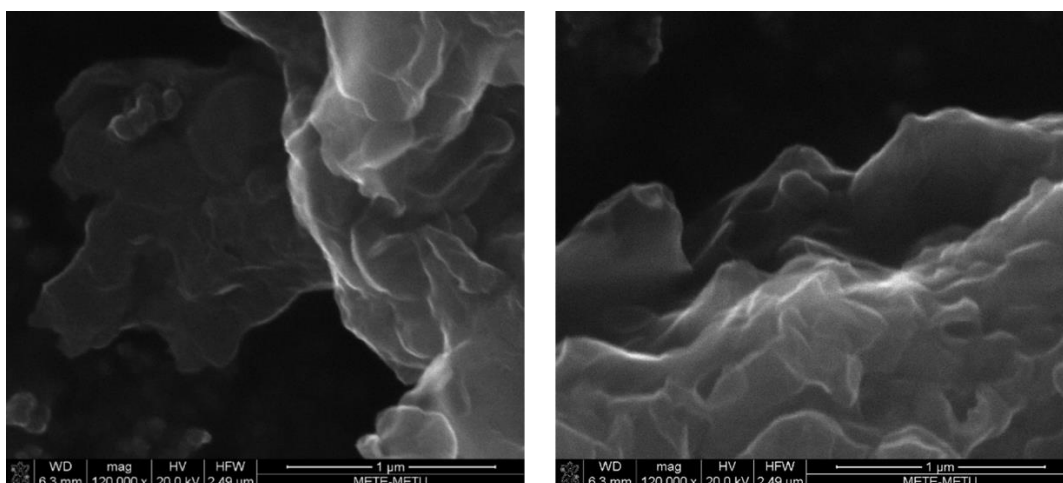


Figure 4.28. The SEM images of graphene particles with 0.25M  $H_2SO_4$ , 0.4M  $HNO_3$ , 0.2M  $NH_4OH$  with 4V and 0.2A (exp16).

XRD spectrum of experiment 16 was given figure 4.29. It is observed that (100) peak is more distinct is experiment 16 which shows the graphene formation.

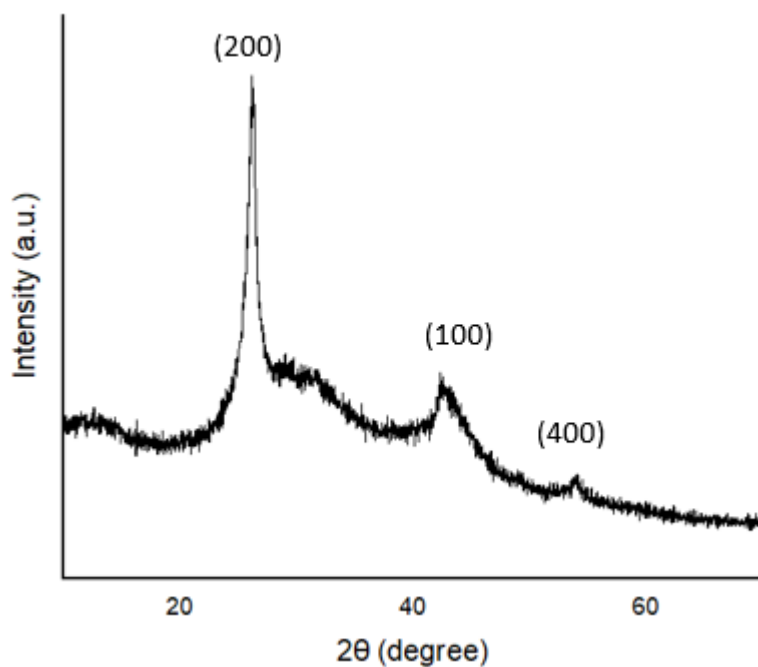


Figure 4.29. XRD spectrum of experiment 16

#### 4.3.4.6. With Antioxidant Agent NaOH

Experiments 11, 12, 13 and 14 were done with antioxidant agent NaOH. These experiments were studied above.

#### 4.3.5. Other Characterizations

Specific surface area was measured with BET analysis for some promising experiments. Figure 4.29 shows the adsorption isotherms of the experiment 4, 7, 13 and 14. Specific surface areas of the experiments were calculated as 27.7 m<sup>2</sup>/g, 24.2 m<sup>2</sup>/g, 3.16 m<sup>2</sup>/g and 110.6 m<sup>2</sup>/g respectively

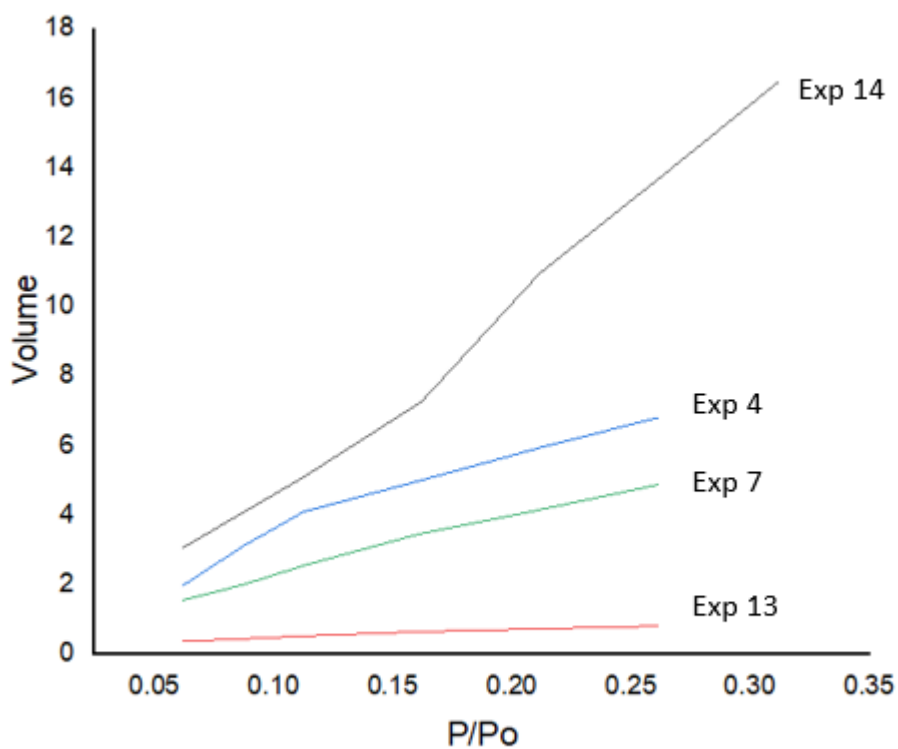


Figure 4.30. BET analysis of experiment 4, 7, 13 and 14.



## CHAPTER 5

### CONCLUSIONS

#### 5.1. Conclusions

- Applied current and potential are more efficient than the concentration of the solution on exfoliation ratio. Current was varied between 0.1 A and 0.6 A and it is optimized at 0.15 A for both the quality and amount of the synthesized graphene. The voltage has important effect on exfoliation rate and its value was optimized at 5.5 V for this study.
- When current decreases, the quality of the graphene powders increases in the same concentration of solution. Flake like structures can be obtained at lower currents.
- Since the ionic radii of  $\text{SO}_4^{2-}$  and  $\text{NO}_3^-$  ions are 0.258 nm and 0.179 nm respectively and the graphene sheets' interplanar spacing is 0.335 nm,  $\text{SO}_4^{2-}$  ions are small enough to fit between graphene layers and large enough to provide efficient exfoliation.
- $\text{OH}^-$  ions leads to  $\text{O}_2^{2-}$  ions and these peroxide ions are highly nucleophilic. These  $\text{O}_2^{2-}$  ions are very efficient in exfoliation process. Optimized molarity of  $\text{H}_2\text{O}_2$  is determined as 0.75M.
- 2 types of surfactants were utilized. CTAB was found to be more efficient than SDS to prevent agglomeration.
- KOH, NaOH,  $\text{H}_2\text{O}_2$  and  $\text{NH}_4\text{OH}$  were used as antioxidant agent. Among them,  $\text{NH}_4\text{OH}$  was the best, since it did not cause any impurity in graphene powders considering that metal ions are considered as impurities in produced graphene. When any antioxidant agent was not used, oxidation was observed more in powders.
- Powders have generally irregular and different shapes like such as flake like powders, spherical powders and equiaxed powders. Among them, flake like powders show properties of graphene.

- It is observed that graphene sheets were oxidized more in acidic solutions when compared to basic solutions. On the other hand, graphene sheets' thickness, particle homogeneity and yielding were better in acidic medium.

## **5.2. Recommendation for Future Work**

- The type of graphite electrode is very important in experiments. If pyrolytic graphite is used in exfoliation process, the quality and yield of graphene would be higher.
- The graphite electrode should be partially confined and isolated in order to make exfoliation process more controllable. Only the tip of the electrode should be exposed to exfoliation process.
- Effect of temperature on reaction rate and powder quality should be considered in the experiments.

## REFERENCES

- [1] A.H. Castro Neto, F. Guinea, N.M.R Peres, K.S. Novoselov, and A.K. Geim, The electronic properties of graphene.
- [2] Kuilla, T., Bhadra, S., Yao, D., Kim, N., Bose, S., & Lee, J. (n.d.). Recent Advances In Graphene Based Polymer Composites. *Progress in Polymer Science*, 1350-1375
- [3] Chen, D.; Tang, L.; Li, J. *Chem. Soc. Rev.* 2010, 39, 3157
- [4] Y. Zhu, S. Murali, W. Cai, X. Li, J. W. Suk, J. R. Potts and R. S. Ruoff, *Adv. Mater.*, 2010, 22, 3906.
- [5] L. J. Cote, J. Kim, V. C. Tung, J. Luo, F. Kim and J. Huang, *Pure Appl. Chem.*, 2011, 83,95.
- [6] J.C. Meyer et al., The structure of suspended graphene sheets, *Nature* 446 (2007) 60.
- [7] Arun Prakash Aranga Raju, *Production and Applications of Graphene and Its Composites*, 2015.
- [8] K. S. Novoselov, A. K. Geim, S. V. Morozov, D. Jiang, Y. Zhang, S. V. Dubonos, I. V. Grigorieva and A. A. Firsov, *Science*, 2004, 306, 666-669
- [9] A. K. Geim and K. S. Novoselov, *Nat Mater*, 2007, 6, 183-191.
- [10] K. I. Bolotin, K. Sikes, Z. Jiang, M. Klima, G. Fudenberg, J. Hone, P. Kim and H. Stormer, *Solid State Communications*, 2008, 146, 351-355

- [11] Joseph Scott Bunch, J. (n.d.). Mechanical and Electrical Properties of Graphene Sheets (p.19).(2008 ed.)
- [12] G.H. Lee et al., High-strength chemical-vapor deposited graphene and grain boundaries, *Science* 340 (2013) 1073.
- [13] I. W. Frank, D. M. Tanenbaum, A. M. van der Zande and P. L. McEuen, *Journal of Vacuum Science & Technology B: Microelectronics and Nanometer Structures*, 2007, 25, 2558-2561.
- [14] A. A. Balandin, S. Ghosh, W. Bao, I. Calizo, D. Teweldebrhan, F. Miao and C. N. Lau, *Nano letters*, 2008, 8, 902-907.
- [15] Falkovsky, L. A. (2008). Optical properties of graphene. *Journal of Physics: Conference Series*, 129, 012004. doi:10.1088/1742-6596/129/1/012004
- [16] R. Nair, P. Blake, A. Grigorenko, K. Novoselov, T. Booth, T. Stauber, N. Peres and A. Geim, *Science*, 2008, 320, 1308-1308.
- [17] Jibrael, R. I., & Mohammed, M. K. (2016). Production of graphene powder by electrochemical exfoliation of graphite electrodes immersed in aqueous solution. *Optik - International Journal for Light and Electron Optics*, 127(16), 6384-6389.
- [18] C. N. R. Rao, A. K. Sood, K. S. Subrahmanyam and A. Govindaraj, *Angewandte Chemie International Edition*, 2009, 48, 7752-7777.
- [19] Y.B. Zhang, Y.W. Tan, H.L. Stormer, P. Kim, Experimental observation of the quantum Hall effect and Berry's phase in graphene, *Nature* 438 (2005) 201.
- [20] H. Yang et al., Graphene Barristor, a Triode Device with a Gate-Controlled Schottky Barrier, *Science* 336 (2012) 1140.

- [21] L. Liao et al., High-speed graphene transistors with a self-aligned nanowire gate, *Nature* 467 (2010) 305.
- [22] M.F. El-Kady, V. Strong, S. Dubin, R.B. Kaner, Laser Scribing of highperformance and flexible graphene-based electrochemical capacitors, *Science* 335 (2012) 1326.
- [23] Y.Q. Wu et al., High-frequency, scaled graphene transistors on diamond-like carbon, *Nature* 472 (2011) 74.
- [24] F. Bonaccorso, Z. Sun, T. Hasan, A.C. Ferrari, Graphene photonics and optoelectronics, *Nat Photonics* 4 (2010) 611.
- [25] J. Wu et al., Organic light-emitting diodes on solution-processed graphene transparent electrodes, *ACS Nano* 4 (2010) 43.
- [26] S. Bae et al., Roll-to-roll production of 30-inch graphene films for transparent electrodes, *Nat. Nanotechnol.* 5 (2010) 574.
- [27] M.F. El-Kady, V. Strong, S. Dubin, R.B. Kaner, Laser Scribing of highperformance and flexible graphene-based electrochemical capacitors, *Science* 335 (2012) 1326.
- [28] S. Choi et al., Friction anisotropy-driven domain imaging on exfoliated monolayer graphene, *Science* 333 (2011) 607.
- [29] Xia, J., Chen, F., Li, J. & Tao, N. Measurement of the quantum capacitance of graphene. *Nat. Nanotechnol.* 4, 505–509 (2009).
- [30] Wang, G. *et al.* Sn/graphene nanocomposite with 3D architecture for enhanced reversible lithium storage in lithium ion batteries. *J. Mater. Chem.* 19, 8378–8384 (2009).

[31] *Maher F. El-Kady, Yuanlong Shao and Richard B. Kaner.* Graphene for batteries, supercapacitors and beyond.

[32] Kou, L. *et al.* Coaxial wet-spun yarn supercapacitors for high-energy density and safe wearable electronics. *Nat. Commun.* 5, 3754 (2014).

[33] Li, Z., Liu, Z., Sun, H. & Gao, C. Superstructured assembly of nanocarbons: fullerenes, nanotubes, and graphene. *Chem. Rev.* 115, 7046–7117 (2015).

[34] Shao, Y., Wang, H., Zhang, Q. & Li, Y. Fabrication of large-area and high-crystallinity photoreduced graphene oxide films via reconstructed two-dimensional multilayer structures. *NPG Asia Mater.* 6, e119 (2014).

[35] Retrieved from: <https://www.graphenea.com/pages/graphene-uses-applications#.XVRE7EXVLIV>

[36] Szabo, T., Szeri, A. & Dekany, I. Composite graphitic nanolayers prepared by self-assembly between finely dispersed graphite oxide and a cationic polymer. *Carbon* 43, 87–94 (2005).

[37] Sasha Stankovich, Dmitriy A. Dikin, Geoffrey H. B. Dommett, Kevin M. Kohlhaas, Eric J. Zimney<sup>1</sup>, Eric A. Stach, Richard D. Piner, SonBinh T. Nguyen & Rodney S. Ruoff. Graphene-based composite materials.

[38] Retrieved from: <https://www.graphene-info.com/graphene-paints>

[39] R.K. Joshia, S. Alwarappanb, M. Yoshimurac, V. Sahajwallaa, Y. Nishinad  
Graphene oxide: the new membrane material

[40] Na Songa, Xueli Gaoa, Zhun Mac, Xiaojuan Wanga, Yi Weia, Congjie Gaoa. A review of graphene-based separation membrane: Materials, characteristics, preparation and applications

- [41] Joonho Lee, N.R. Aluru. Water solubility driven separation of gases using graphene membrane
- [42] K.S. Kim, Y. Zhao, H. Jang, S.Y. Lee, J.M. Kim, K.S. Kim, et al., Large-scale pattern growth of graphene films for stretchable transparent electrodes, *Nature* 457 (2009) 706-716.
- [43] A. Guermoune, T. Chari, F. Popescu, S.S. Sabri, J. Guillemette, H.S. Skulason, T. Szkopek, M. Siaj, Chemical vapor deposition synthesis of graphene on copper with methanol, ethanol, and propanol precursors, *Carbon* 49 (2011) 4204-4210.
- [44] M. Borysiak. Graphene synthesis by CVD on copper substrates. The 2009 NNIN REU Research Accomplishments (2009) 70-71.
- [45] H. Tetlow, J. Posthuma de Boer, I.J. Ford, D.D. Vvedensky, J. Coraux, L. Kantorovich, Growth of epitaxial graphene: Theory and experiment.
- [46] F. Hiebel, P. Mallet, F. Varchon, L. Magaud, J.Y. Veuille, Graphene–substrate interaction on 6H-SiC (000 $\bar{1}$ ): a scanning tunneling microscopy study, *Phys. Rev. B* 78 (2008) 153412.
- [47] T.A. Land, T. Michely, R.J. Behm, J.C. Hemminger, G. Comsa, STM investigation of single layer graphite structures produced on Pt (111) by hydrocarbon decomposition, *Surf. Sci.* 264 (1992) 261–270.
- [48] O.V. Yazyev, Emergence of magnetism in graphene materials and nanostructures, *Rep. Progr. Phys.* 73 (2010) 056501.
- [49] H. Tetlow et al. / *Physics Reports* 542 (2014) 195–295 199.
- [50] K.S. Novoselov, A.K. Geim, S.V. Morozov, D. Jiang, Y. Zhang, S.V. Dubonos, I.V. Grigorieva, A.A. Firsov, Electric field effect in atomically thin carbon films, *Science* 306 (2004) 666–669.

- [51] R. Van Noorden, Production: beyond sticky tape, *Nature* 483 (2012) S32–S33.
- [52] D.R. Dreyer, S. Park, C.W. Bielawski, R.S. Ruoff, The chemistry of graphene oxide, *Chem. Soc. Rev.* 39 (2010) 228–240.
- [53] S. Stankovich, D.A. Dikin, R.D. Piner, K.A. Kohlhaas, A. Kleinhammes, Y. Jia, Y. Wu, S.T. Nguyen, R.S. Ruoff, Synthesis of graphene-based nanosheets via chemical reduction of exfoliated graphite oxide, *Carbon* 45 (2007) 1558–1565.
- [54] H. Shin, K.K. Kim, A. Benayad, S. Yoon, H.K. Park, I. Jung, M.H. Jin, H. Jeong, J.M. Kim, J. Choi, Y.H. Lee, Efficient reduction of graphite oxide by sodium borohydride and its effect on electrical conductance, *Adv. Funct. Mater.* 19 (2009) 1987–1992.
- [55] M.J. Fernández-Merino, L. Guardia, J.I. Paredes, S. Villar-Rodil, P. Solís-Fernández, A. Martínez-Alonso, J.M.D. Tascón, Vitamin C is an ideal substitute for hydrazine in the reduction of graphene oxide suspensions, *J. Phys. Chem. C* 114 (2010) 6426–6432.
- [56] C. Vallés, J. David Núñez, A.M. Benito, W.K. Maser, Flexible conductive graphene paper obtained by direct and gentle annealing of graphene oxide paper, *Carbon* 50 (2012) 835–844.
- [57] H.J. Han, Y.N. Chen, Z.J. Wang, Effect of microwave irradiation on reduction of graphene oxide films, *RSC Adv.* 5 (2015) 92940–92946.
- [58] D.C. Marcano, D.V. Kosynkin, J.M. Berlin, A. Sinitskii, Z. Sun, A. Slesarev, L.B. Alemany, W. Lu, J.M. Tour, Improved synthesis of graphene oxide, *ACS Nano* 4 (2010) 4806–4814.

- [59] S. Wang, Y. Zhang, N. Abidi, L. Cabrales, Wettability and surface free energy of graphene films, *Langmuir* 25 (2009) 11078–11081.
- [60] Y. Hernandez, V. Nicolosi, M. Lotya, F.M. Blighe, Z. Sun, S. De, I.T. McGovern, B. Holland, M. Byrne, Y.K. Gun'Ko, J.J. Boland, P. Niraj, G. Duesberg, S. Krishnamurthy, R. Goodhue, J. Hutchison, V. Scardaci, A.C. Ferrari, J.N. Coleman, High-yield production of graphene by liquid-phase exfoliation of graphite, *Nat. Nanotechnol.* 3 (2008) 563–568.
- [61] A. Ciesielski, P. Samori, Graphene via sonication assisted liquid-phase exfoliation, *Chem. Soc. Rev.* 43 (2014) 381–398.
- [62] A. O'Neill, U. Khan, P.N. Nirmalraj, J. Boland, J.N. Coleman, Graphene dispersion and exfoliation in low boiling point solvents, *J. Phys. Chem. C.* 115 (2011) 5422–5428.
- [63] K. Parvez, S. Yang, X. Feng, K. Müllen, Exfoliation of graphene via wet chemical routes, *Synth. Met.* 210 (Part A) (2015) 123–132.
- [64] M.V. Antisari, A. Montone, N. Jovic, E. Piscopiello, C. Alvani, L. Piloni, Low energy pure shear milling: a method for the preparation of graphite nanosheets, *Scr. Mater.* 55 (2006) 1047–1050.
- [65] W. Zhao, M. Fang, F. Wu, H. Wu, L. Wang, G. Chen, Preparation of graphene by exfoliation of graphite using wet ball milling, *J. Mater. Chem.* 20 (2010) 5817.
- [66] M. Ullah, M.E. Ali, S.B. Abd Hamid, Surfactant-assisted ball milling: a novel route to novel materials with controlled nanostructure – a review, *Rev. Adv. Mater. Sci.* 37 (2014) 1–14.

[67] N. Liu, F. Luo, H. Wu, Y. Liu, C. Zhang, and J. Chen, "One-Step Ionic-Liquid-Assisted Electrochemical Synthesis of Ionic-Liquid-Functionalized Graphene Sheets Directly from Graphite," *Adv. Funct. Mater.*, vol. 18, no. 10, pp. 1518–1525, May 2008.

[68] J. Liu, *Graphene-Based Composites for Electrochemical Energy Storage*, Springer Nature Singapore Pte Ltd. 2017.

[69] A. M. Abdelkader, A. J. Cooper, R. A. W. Dryfe, I. A. Kinlocha, How to get between the sheets: a review of recent works on the electrochemical exfoliation of graphene materials from bulk graphite.

[70] J. Lu, J.X. Yang, J.Z. Wang, A.L. Lim, S. Wang, K.P. Loh, One-pot synthesis of fluorescent carbon nanoribbons, nanoparticles, and graphene by the exfoliation of graphite in ionic liquids. *ACS Nano* 3, 2367–2375 (2009).

[71] J.C. Goak, S.H. Lee, J.H. Han, S.H. Jang, K.B. Kim, Y. Seo, Y.S. Seo, N. Lee, Spectroscopic studies and electrical properties of transparent conductive films fabricated by using surfactant-stabilized single-walled carbon nanotube suspensions, *Carbon* 49 (2011) 4301-4313.

[72] M. Alanyahoğlu, J.J. Segura, J.O. Solè, N.C. Pastor, The synthesis of graphene sheets with controlled thickness and order using surfactant-assisted electrochemical processes, *Carbon* 50 (2012) 142-153.

[73] Parvez, K.; Wu, Z. S.; Li, R.; Liu, X.; Graf, R.; Feng, X.; Mullen, K. Exfoliation of Graphite into Graphene in Aqueous Solutions of Inorganic Salts. *J. Am. Chem. Soc.*, 2014, 136, 6083- 6091.

[74] J. Wang, K. K. Magnga, Q. Bao and K. P. Loh, *J. Am. Chem. Soc.*, 2011, 133, 8888–8891

[75] B. Marta, C. Leordean, T. Istvan, I. Botiz and S. Astilean, *Appl. Surf. Sci.*, 2016, 363, 613–618.

[76] Chien-Te Hsieh, Jen-Hao Hsueh, Electrochemical exfoliation of graphene sheets from a natural graphite flask in the presence of sulfate ions at different temperatures.

[77] Ching-Yuan Su, Ang-Yu Lu, Yanping Xu, Fu-Rong Chen, Andrei N Khlobystov, Lain-Jong Li, High-quality thin graphene films from fast electrochemical exfoliation.

[78] Rao, K. S.; Senthilnathan, J.; Liu, Y. F.; Yoshimura, M. Role of Peroxide Ions in Formation of Graphene Nanosheets by Electrochemical Exfoliation of Graphite. *Sci. Rep.*, 2014, 4, 4237.

[79] Sumanta Kumar Sahoo, Archana Malli, Simple, Fast and Cost-Effective Electrochemical Synthesis of Few Layer Graphene Nanosheets

[80] P. Khanra, T. Kuila, S. H. Bae, N. H. Kim and J. H. Lee, *J. Mater. Chem.*, 2012, 22, 24403–24410.

[81] J.Z. Wang, K.K. Manga, Q.L. Bao, K.P. Loh, High-yield synthesis of few-layer graphene flakes through electrochemical expansion of graphite in propylene carbonate electrolyte. *J. Am. Chem. Soc.* 133, 8888–8891 (2011)

[82] C. Y. Yang, C. L. Wu, Y. H. Lin, L. H. Tsai, Y. C. Chi, J. H. Chang, C. I. Wu, H. K. Tsai, D. P. Tsai and G. R. Lin, *Opt. Mater. Express*, 2013, 3, 1893–1905.

[83] S. Ravula, S. Baker, G. Kamath and G. Baker, *Nanoscale*, 2015, 7, 4338–4353.

[84] Dasent, p. 78; H.D.B. Jenkins and K.P. Thakur, *J. Chem. Educ.*, 56, 576 (1979).

[85] Kaneko, K., Ishii, C., & Ruike, M. (1992). Origin of superhigh surface area and microcrystalline graphitic structures of activated carbons. *Carbon*, 30(7), 1075-1088.

[86] Centeno, T. A., & Stoeckli, F. (2010). The assessment of surface areas in porous carbons by two model-independent techniques, the DR equation and DFT. *Carbon*, 48(9), 2478-2486.

[87] Yan Wang-Zhiqiang Shi-Yi Huang-Yanfeng Ma-Chengyang Wang-Mingming Chen-Yongsheng Chen - *The Journal of Physical Chemistry C*, 113, 13103-13107-2009

[88] Texter, J. (2014). Graphene dispersions. *Current Opinion in Colloid & Interface Science*, 19(2), 163-174. Doi: 10.1016/j.cocis.2014.04-004

[89] Pu, N.-W., Wang, C.-A., Liu, Y.-M., Sung, Y., Wang, D.-S., & Ger, M.-D. (2012). Dispersion of graphene in aqueous solutions with different types of surfactants and the production of graphene films by spray or drop coating. *Journal of the Taiwan Institute of Chemical Engineers*, 43(1), 140–146. doi: 10.1016/j.jtice.2011.06.012

[90] Çiplak, Zafer, et al. “Investigation of Graphene/Ag Nanocomposites Synthesis Parameters for Two Different Synthesis Methods.” *Fullerenes, Nanotubes and Carbon Nanostructures*, vol. 23, no. 4, Oct. 2014, pp. 361–370., doi:10.1080/1536383x.2014.894025.

[91] Siburian, R., Sihotang, H., Raja, S. L., Supeno, M., & Simanjuntak, C. (2018). New Route to Synthesize of Graphene Nano Sheets. *Oriental Journal of Chemistry*, 34(1), 182–187. doi: 10.13005/ojc/340120





